11-13-2017

Evidence of Subglacial Brine Inflow and Wind-Induced Mixing from High Resolution Temperature Measurements in Lake Bonney, Antarctica

Jade Lawrence
Louisiana State University and Agricultural and Mechanical College

EVIDENCE OF SUBGLACIAL BRINE INFLOW AND WIND-INDUCED MIXING FROM HIGH RESOLUTION TEMPERATURE MEASUREMENTS IN LAKE BONNEY, ANTARCTICA

A Thesis

Submitted to the Graduate Faculty of
Louisiana State University and
Agricultural and Mechanical College
In the partial fulfillment of the
requirements for the degree of
Master of Science

in

The Department of Geology and Geophysics

by
Jade Lawrence
B.A., University of California Santa Barbara, 2012
December 2017

To my friends K, J, and A-
I couldn't have done it without you

But then patch me right back to Lake Bonney,
Patch me whatever the price;
The ice on the lake
Doesn't hurry, or wait,
And it might be Paradise.

-Bill Manhire, *Deep Field Song*

ACKNOWLEDGMENTS

This work was funded by the National Science Foundation LTER grant 1115245. Many thanks to the C-511 field teams in 2015 and 2016, as well as the science support staff in Antarctica that made it possible. Long term records would not have been possible without the MCM LTER and the many field teams who came before me. Special thanks to Krista Myers and Luke Winslow for their feedback. Additional thanks go to Kathy Welch, Berry Lyons, Robert Spigel, Erin Pettit, and other MCM scientists who shared data or feedback. Thanks to my advisor, Peter Doran, for the opportunities.

LIST OF TABLES

LIST OF FIGURES

TABLE OF CONTENTS

ABSTRACT

Hypersaline brine beneath Taylor Glacier enters proglacial West Lobe Lake Bonney (WLB) subglacially as well as from Blood Falls, a surface discharge point at the Taylor Glacier terminus. The brine strongly influences the water column of WLB. Because of the extremely high salinities below the chemocline in WLB, density is determined almost entirely by salinity and temperature can be used as a passive tracer. Cold brine intrusions enter WLB at the glacier face and intrude in to the water column at the depth of neutral buoyancy, where they can be identified by anomalously cold temperatures at that depth. This study is the first to definitively identify subglacial brine intrusions in WLB, since the absence of an open water moat in the winter prevents brine entry from the surface at Blood Falls. High resolution thermistors and CTDs deployed year-round beneath the perennial ice cover demonstrate that brine intrusions can influence the thermal stratification of the water column near the glacier terminus for the majority of the year, and that the effects diminish with distance from the glacier terminus. High volumes of brine inflow alter the density stratification of the water column at the depth of the intrusion and cause turbulent mixing near the glacier terminus. High resolution measurements also reveal internal water movements associated with katabatic wind events, a novel finding that challenges long held assumptions about the stability of the WLB water column. The long term records of Blood Falls flow and of temperature anomalies in WLB indicate that brine release from the subglacial system has been a persistent feature in the region for decades, with implications for the geochemistry and biology of WLB.

1. INTRODUCTION

The McMurdo Dry Valleys (MDVs) are the largest ice-free region in Antarctica, with a combined area of 4500 km^2 (Levy, 2013). Ice-free conditions are maintained by the presence of the Transantarctic Mountains, which create a precipitation shadow and prevent the flow of the East Antarctic Ice Sheet into the valleys (Fountain et al., 2010). Taylor Valley has been the site of extensive study by the McMurdo Long Term Ecological Research group (MCM LTER) since the early 1990s. Valley bottom mean annual temperatures in the MDVs range from -14.8°C to -30°C (Doran et al., 2002), and average annual precipitation (as snow only) is less than 50 mm water equivalent (Fountain et al., 2010). Low precipitation relative to potential evaporation, low surface albedo, and dry katabatic winds create extremely arid conditions in the valleys (Clow et al., 1998). This cold desert environment is often used as an analog for extreme environments on Mars or other planets (Doran et al., 1998; Doran et al., 2004; Holt et al., 2006; Dachwald et al., 2014; Mikucki et al., 2015).

Closed-basin lakes beneath thick perennial ice covers persist in the MDVs due to a combination of unique climatic factors. The short austral summer is warm enough for liquid water inflow into the lakes from glacial melt, yet not warm enough to melt the entire ice cover. An equilibrium ice thickness is maintained by a balance between year-round ablation and new ice forming at the bottom of the ice cover (Obryk et al., 2016). Freezing at the base of the ice cover releases latent heat that offsets the heat loss to the atmosphere through the ice (Spigel and Priscu, 1998). The protection of the ice cover, combined with extreme density stratification from strong salinity gradients, create highly stable water columns in most of the Dry Valley lakes (Spigel and Priscu, 1998). Lake temperatures respond to seasonal and annual variations in weather, climate, and lake levels in the MDVs, but much less than in temperate lakes (Spigel and Priscu, 1998).

Previous studies have concluded that the thick perennial ice cover prevents turbulent mixing from wind as seen in most other lakes (Wharton, 1993; Spigel and Priscu, 1998). The absence of basin-scale stirring, turbulent mixing from wind, and convective overturn has important implications for microbial life in the lake (Vincent, 1981). Stability in Dry Valley lakes ranges from similar to the stability of summer thermoclines of freshwater lakes (Lake Hoare) to ~1000 times more stable in the extreme stratification of the West Lobe Bonney chemocline (Spigel and Priscu, 1998). However, summer surface seiches have been observed in some Dry Valley lakes caused either by high winds (Lake Vanda; Heine, 1971) or possibly by diurnal stream input (Lake Hoare; Castendyk et al., 2015).

Lake Bonney in Taylor Valley is unique within the MDVs due to the extreme salinities below the chemocline (Spigel and Priscu, 1998) and due to the direct input of hypersaline, anoxic, and iron-rich subglacial brine that exists beneath Taylor Glacier (Mikucki et al., 2004). Subglacial aquatic environments in Antarctica have attracted significant attention in recent years (Siegert et al., 2013). The brine system beneath Taylor Glacier is unique because it lies beneath relatively thin ice, and because it is more accessibly studied at Blood Falls, a surface brine outlet at the northern terminus of Taylor Glacier. The liquid brine system beneath Taylor Glacier has implications for cold-based glacier systems (Badgeley et al., 2017) and our understanding of the complex geochemical history of Lake Bonney (Poreda et al., 2004; Doran et al., 2014; Hall et al., 2017).

1.1 Study Area: Lake Bonney

Lake Bonney is the westernmost lake in Taylor Valley. The lake is divided into two lobes separated by a narrow sill (Spigel and Priscu, 1998). West Lobe of Lake Bonney (WLB) abuts the terminus of Taylor Glacier, which flows from Taylor Dome on the polar plateau (Figure 1). The ice cover on both lobes ranges from 3-5 m (Spigel and Priscu, 1998). Maximum water depth in both lobes is approximately 40 m (Spigel and Priscu, 1998; unpublished data).

The interaction of WLB with the Taylor Glacier terminus causes WLB to be significantly colder and more thermally variable than the East Lobe of Lake Bonney (ELB). Although some water is exchanged between ELB and WLB (Spigel and Priscu, 1998; Doran et al., 2014) they are often treated as separate water bodies. Isotopic analysis and geochemical modeling suggest that the two lobes reconnected approximately 200 years ago, and that lake levels have continued rising to the present day

(Hall et al., 2017; Doran et al., 2014; Poreda et al., 2004). This timeline is supported by the first observations of the region by Robert Scott in 1903 (Scott, 1905). Scott's measurement of the width of the narrows was later converted to an estimated water depth of just a few meters (Chinn, 1993), compared to a depth of ~15 m in 2009 (Spigel et al., in revision).

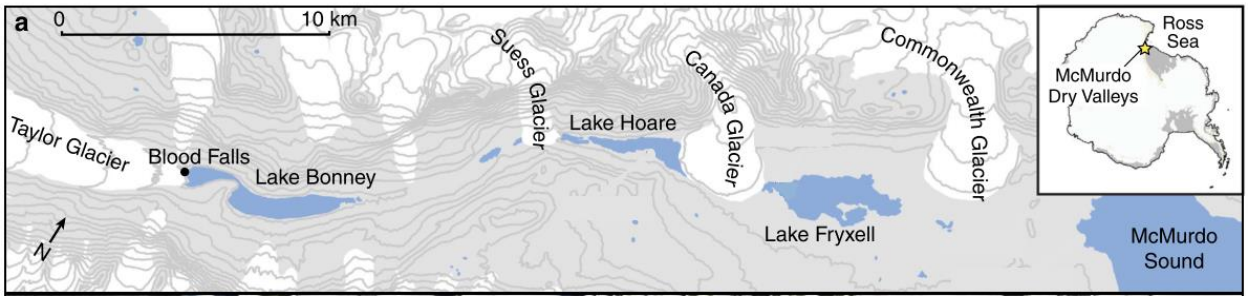

Figure 1. Map of Taylor Valley showing Lakes Bonney, Hoare, and Fryxell. The inset shows the location of the McMurdo Dry Valleys on the Antarctic continent. Adapted from Mikucki et al., 2015.

The steep salinity gradient below the chemocline in WLB results in a highly stratified and extremely stable water column. Temperature exerts such a small effect on density in WLB that it can be used as a passive tracer to identify water movements in the highly saline water below the chemocline (Spigel and Priscu, 1998). This scenario is the opposite in freshwater lakes, where density is primarily determined by temperature and small changes in conductivity can be used to trace water movements. The water column above the chemocline in WLB contains relatively fresh, warm water. The temperature maximum in WLB of ~3°C occurs above the chemocline at 9-10 m depth due to solar energy that penetrates the thick ice cover and is then stored at depth by the salt gradient (Hoare et al., 1964; Shirtcliffe and Benseman, 1964). The bottom of WLB is near -5°C, but due to the high salt content this is still well above the freezing point (Spigel and Priscu, 1998; Spigel et al., in revision). The high concentration of salts in the bottom waters of WLB stems from a period of aridity 6-11 ky B.P. that evaporated most or all of WLB (Hendy, 2000). Typical profiles for temperature, density, and salinity for WLB are shown in Figure 2.

The depth of the chemocline in WLB is determined by the elevation of the sill between the two lobes. Salty, dense water that extends above the level of the sill in the west lobe is transported over the sill into the east lobe in a phenomenon known as "chemocline leakage" (Doran et al., 2014). This net west-east transport through the narrows maintains a sharp chemocline gradient in the west lobe and a peak in stability at the elevation of the sill, compared to a more diffuse chemocline in ELB (Spigel and Priscu, 1998).

The extreme density stratification in WLB inhibits turbulent mixing beneath the ice cover, and turbulence has been observed in WLB only under specific circumstances. Turbulent mixing in WLB was observed when a high streamflow event caused instability in the water column above the chemocline (Foreman et al., 2004). Turbulent flow has been observed in the narrows between the two lobes, probably due to complex exchange flow (Spigel and Priscu, 1998). Additionally, salinity and temperature profiles in the region of WLB directly adjacent to the glacier face exhibit static instability (Spigel et al., in revision). Because the fresh water above the chemocline is >0°C and the cold water below the chemocline is extremely saline, ambient water temperatures exceed freezing temperatures above and below the chemocline and the glacier face is melting at all depths where it interacts with the water column. Meltwater intrusions above the chemocline rise buoyantly to the bottom of the ice cover and may initiate basin-wide circulation above the chemocline extending into the narrows and the east lobe (Spigel et al., in revision). Meltwater intrusions below the chemocline do not buoyantly rise to the surface, but instead propagate in to the lake as a series of nearly horizontal intrusions that are evident in fine-scale measurements near the glacier as small oscillations in the temperature and salinity profiles (Spigel et al., in revision). Overturning occurs in these oscillatory layers closest to the glacier, but quickly evolves into a stable configuration with distance from the glacier face (Spigel et al, in revision).

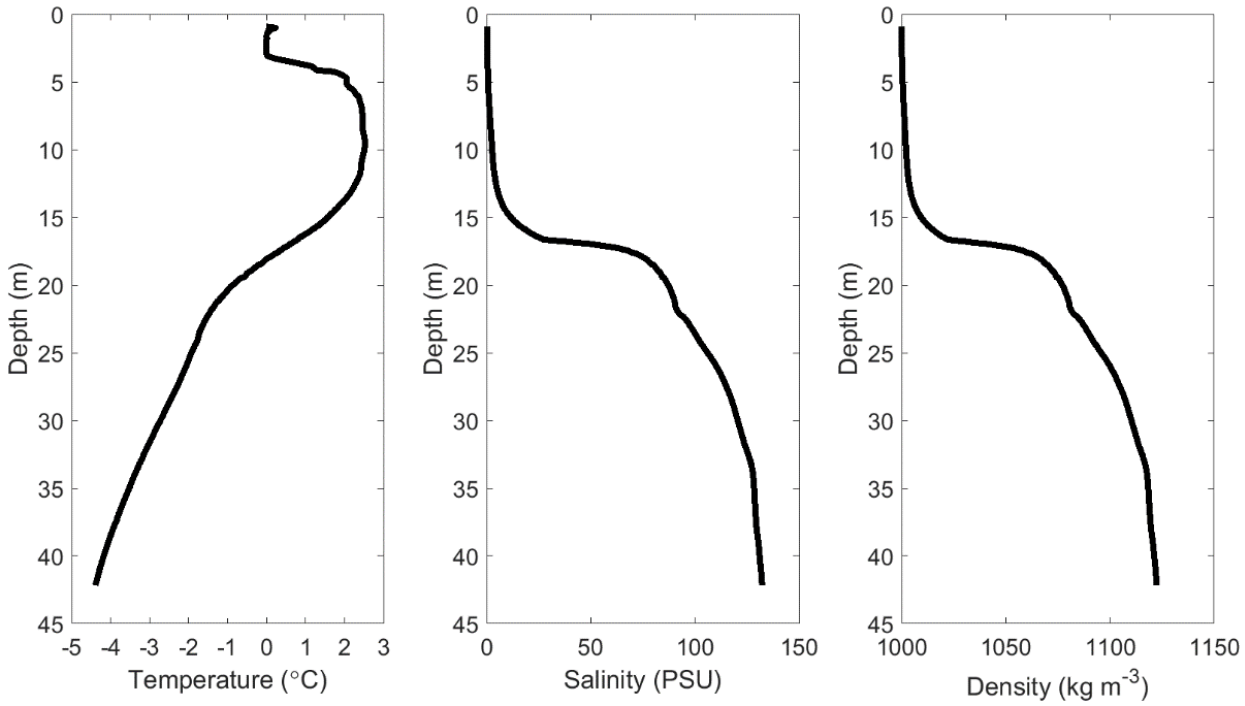

Figure 2. Typical profiles of temperature, salinity, and density in WLB from a CTD cast in December 2014. The similar shape of the salinity and density profiles reflects the degree to which salinity determines density.

1.2 Blood Falls and the Larger Brine System beneath Taylor Glacier

Blood Falls is a surface outflow feature of subglacial brine that creates a visible red stain on the northern end of the terminus of Taylor Glacier and the adjacent ice of WLB (Figure 3). Although Robert Scott explored Lake Bonney and the surrounding areas in his 1903 expedition, the first observation of Blood Falls was not made until 1911 by Griffith Taylor (Taylor, 1922). Black et al. (1965) deduced that the red coloration of Blood Falls was caused by iron oxides, not from red algae as hypothesized by Taylor (1922). Iron in the subglacial brine is reduced at depth, but stains the ice red once it oxidizes by exposure to air at the surface. The brine is hypersaline, anoxic, and has high concentrations of ferrous iron, silica, and sulfate (Mikucki et al., 2009). It supports a metabolically active microbial community that influences subglacial weathering (Mikucki et al., 2015). The brine density at the Blood Falls outflow is 1100 kg m^{-3} (Keys, 1979) and can remain liquid below -7°C (Badgeley et al., 2017). The primary brine discharge point at the north end of the Taylor Glacier terminus has remained in roughly the same position since early observations despite movement of the glacier (Badgeley et al., 2017). The brine outflow is episodic and highly variable, though Keys (1979) estimated that Blood Falls discharge averages 2,000 m^3 per year based on the volume of saline icing visible after discharge events. The hydrologic mechanisms controlling brine release have only recently been discovered (Badgeley et al., 2017).

Despite its novelty and importance to the hydrology of the region, no comprehensive records exist of Blood Falls flow events. Flow events were reported in the first papers describing the phenomenon (Black et al., 1965; Black, 1969; Keys, 1979), and other published accounts of active flow events at Blood Falls are limited to the 1990-1991 austral summer season (Spigel and Priscu, 1998; Mikucki et al., 2004), and the austral summers of 2000-2004 (Mikucki and Priscu, 2007; Mikucki et al, 2009).

The Blood Falls outflow and WLB are hydrologically connected to a larger system of hypersaline brine that exists beneath Taylor Glacier. Hubbard et al. (2004) used ice penetrating radar and thermodynamic modelling to suggest that hypersaline brine existed in a subglacial zone 3-6 km up Taylor Glacier from the terminus and 400-1000 m across the glacier. That area coincided with an extensive

topographic overdeepening of 80 m below sea level at 5.75 km up glacier from the terminus (Hubbard et al., 2004). The presence of liquid brine was confirmed by a recent airborne transient electromagnetic (AEM) survey, where the lowest resistivity values beneath Taylor Glacier coincided with the same topographic overdeepening (Mikucki et al., 2015). The AEM survey shows that there is liquid brine or brine saturated sediments underlying all of Taylor Glacier from the terminus until at least ~6 km up glacier (Mikucki et al., 2015). The estimated volume of brine saturated sediments below Taylor Glacier is 1.5 km^3 (Mikucki et al., 2015). The volume of liquid brine is unknown given the unconstrained porosity of the subglacial sediments, but likely exceeds the volume of all the Taylor Valley lakes combined (Mikucki et al., 2015).

Figure 3. Blood Falls at the northern end of the terminus of Taylor Glacier. Photo by Hassan Basagic.

Previous thermodynamic models of Taylor Glacier indicated that the basal temperatures were well below the pressure melting point of ice, so Taylor Glacier has been primarily considered a cold-based glacier that is frozen to its bed (Robinson, 1984; Hubbard et al., 2004; Kavanaugh and Cuffey, 2009). These models suggested that basal sliding does not occur in Taylor Glacier, and that glacier flow was controlled by deformation of subfreezing ice (Kavanaugh and Cuffey, 2009). Pettit et al. (2014) suggested that the elevated surface velocities (compared to laminar flow for clean, homogenous, isotropic ice) of Taylor Glacier at the terminus are due to deformation of the debris rich basal ice layer rather than basal sliding. The authors concluded that the basal ice layer must be 10-15 m thick and 20-40 times softer than clean Holocene-age glacier ice (Pettit et al., 2014). Chloride, calcium, and sulfate ions increase ice softness (Paterson, 1991: Cuffey et al., 2000a) by concentrating in and increasing the thickness of liquid water films along ice-crystal boundaries (Paren and Walker, 1971; Pettit et al., 2014). Salts in the brine-saturated sediments could contribute to the increased softness of the debris rich basal ice. However, since the airborne resistivity data confirms the presence of unfrozen water beneath Taylor Glacier (due to the freezing point being depressed by salts), basal sliding might also occur in the terminus region of Taylor Glacier (Mikucki et al., 2015).

The brine is most likely a remnant feature from an incursion of marine water into the MDVs from the Ross Sea during the Miocene, when the MDVs were a series of fjords (Elston and Bressler, 1981). When the marine waters retreated, a remnant sea remained in the depression near the Taylor Glacier terminus and became cryoconcentrated over time. Taylor Glacier advanced in the late Pliocene or Pleistocene and trapped the hypersaline brine beneath it (Marchant et al., 1993). The subsequent advances and retreats of Taylor Glacier and changes in lake levels since the Pleistocene have undoubtedly modified the chemistry of the subglacial brine (Mikucki et al., 2004). Multiple lines of evidence support the hypothesis that the brine is of marine origin. The major ion ratios of Na:Cl and Cl:Br of Blood Falls discharge and of the bottom waters of WLB are similar to seawater (Mikucki et al., 2004). Blood Falls discharge is enriched in magnesium and calcium relative to seawater, probably due to cryoconcentration of the brine and subglacial weathering (Mikucki et al., 2004). The majority of bacteria isolated from Blood Falls outflow is phylogenetically related to marine lineages (Mikucki and Priscu, 2007). Additionally, low ^{36}Cl values in Blood Falls and the deep waters of WLB are compatible with the primary chloride source being isotopically "dead" ancient marine salts (Lyons et al., 1998).

1.3 Hydrologic Mechanisms Controlling Brine Flow

A new study by Badgeley et al. (2017) demonstrates that the subglacial brine is not in thermal equilibrium with the glacier ice because the ambient temperature of the brine (-7°C) is 10°C warmer than the surrounding glacier ice (-17°C). The brine remains liquid as it travels down the glacier by partially freezing, releasing latent heat that slightly warms the surrounding glacier ice and cryoconcentrating the remaining liquid brine, which further reduces the freezing point (Badgeley et al., 2017). Liquid brine pockets are advected towards the terminus by glacier flow (3-4 m a^{-1}; Pettit et al., 2014). Badgeley et al. (2017) used subglacial hydraulic potential modeling to determine that deeply incised supraglacial meltwater valleys in the terminus region are responsible for routing subglacial brine flow along specific pathways at the bed. The authors identified multiple englacial brine pathways converging at the north end of the terminus, consistent with the Blood Falls discharge location, as well as brine pathways routing towards the southern end of the glacier and towards the middle of the glacier terminus (Badgeley et al., 2017).

The northern brine pathway terminates in a pressurized englacial brine system in the Blood Falls region (Badgeley et al., 2017). The brine is injected in to englacial basal crevasses, and is released at Blood Falls when a surface crevasse connects with the pressurized liquid brine in the basal crevasse (Badgeley et al., 2017). Physical barriers and differences in surface topography prevent the formation of a similar system in the southern part of the terminus, and the southern and middle brine pathways are expected to flow directly in to Lake Bonney (Badgeley et al., 2017).

1.4 Effect of Subglacial Brine on WLB

The presence of brine underneath Taylor Glacier has important implications for subglacial weathering and the geochemistry of Lake Bonney. Bacterial isolates from Blood Falls outflow are closely related to bacteria that metabolize iron and sulfur (Mikucki and Priscu, 2007). Subsurface microbial processes liberate ions such as iron and silica from the underlying bedrock, which enter Lake Bonney and influence surface ecosystem processes (Mikucki et al., 2015). The subglacial brine environment is also a source of dissolved organic carbon (DOC), either remnant from before the isolation of the brine or from extant subglacial microbial activity (Mikucki et al., 2004). Blood Falls outflow is an important source of DOC for heterotrophic bacteria in Lake Bonney (Mikucki et al., 2004). The stable isotopic geochemistry of Blood Falls is very similar to the hypolimnion of WLB, suggesting that they are closely related (Lyons et al., 2005).

The subglacial brine system beneath Taylor Glacier strongly influences WLB via direct Blood Falls outflow into the lake and through subglacial brine discharge entering the water column beneath the ice cover. Subglacial brine discharge has been proposed as a possible mechanism for brine entry in to Lake Bonney by other researchers (Keys, 1979; Spigel and Priscu, 1998; Doran et al., 2014; Badgeley et al., 2017; Spigel et al., in revision). Keys (1979) hypothesized that subterranean brine flow might occur through a gap in the confining permafrost. Spigel and Priscu (1998) noted that in October 1991, water samples collected between 20 and 25 m depth contained "turbid, reddish iron-oxide-rich water" that had

not been previously observed. The iron in the 1991 water samples was reduced at depth and developed the red coloration upon exposure to air (Mikucki et al., 2004). Blood Falls discharged large amounts of saline brine during the summer of 1990-1991, so the authors hypothesized that the reddish water at depth was “from an intrusion layer that originated at the face of the Taylor Glacier, its source being either an underflow from the well-documented red, saline surface discharge, or possibly a submerged outlet in the glacier face.” CTD profiles from the 2008-2009 ENDURANCE (Environmentally Non-Disturbing Under-ice Robotic Antarctic Explorer) mission (Spigel et al., in revision) showed that anomalously cold water of similar density to Blood Falls brine extended from the submerged glacier face for several hundred meters into the lake, indicative of cold brine entering the lake subglacially and travelling through the lake at the depth of neutral buoyancy.

In this study, thermistors and CTDs deployed year-round beneath the ice cover are used to assess the thermal variability of WLB throughout the year and to identify subglacial brine intrusions through anomalously cold temperatures at specific depths. Frequency analysis of high resolution CTD measurements is performed to identify periodic motion within WLB water column. Near-glacier CTD profiles from the ENDURANCE mission provide insight on the behavior of brine inflows as they enter the water column. The larger context of brine release into WLB as a long term, ongoing process is elucidated by long term records of CTD profiles in WLB and of surface brine flow at Blood Falls.

2. METHODS

2.1 High Resolution Thermistors and CTDs

Two custom RBRconcerto T10 thermistor strings were deployed beneath the ice cover in WLB from December 2014 - November 2015 at Locations A and B in Figure 4. In November 2015 they were relocated towards the center of the glacier terminus to Locations C and D in Figure 4. Thermistor depths and locations are listed in Table 1. In November 2015 two RBRconcerto CTDs were deployed at 18 and 23 m depth at Location C.

The thermistor strings contain ten thermistors each, spaced at 1.44 m intervals. Three thermistors failed and were deleted from the data presented here (Table 1). The thermistors have an accuracy of ±0.002°C. The CTDs have an accuracy of ±0.002°C for temperature and ±0.003 mS cm^{-1} for conductivity. The sampling rate for the thermistors was 15 seconds in 2014-2015 (subsampled to 1 minute) and 1 minute in 2015-2016. The sampling rate of the CTDs in 2015-2016 was 1 minute. Wavelet analysis was performed on density calculated from the CTD data using the Morlet wavelet according to Torrence and Compo (1998).

Figure 4. Satellite image of WLB featuring the locations of the LTER CTD casts (E), thermistor strings (A-D), and Blood Falls. Image from Google Earth (©2017 Google, DigitalGlobe).

Table 1. Thermistor sensor depths and locations in Figure 4. The sensor depths in red indicate a thermistor that failed and was deleted from the data set.

Thermistor	West 2014-2015	East 2014-2015	West 2015-2016	West 2015-2016 CTDs	East 2015-2016
Location in Figure 4	A	B	C	C	D
Sensor Depths (m)	12.13	11.66	12.13	18	11.63
	13.57	13.10	13.57	23	13.07
	15.01	14.54	15.01		14.51
	16.45	15.98	16.45		15.95
	~~17.89~~	17.42	~~17.89~~		17.39
	19.33	18.86	19.33		18.83
	20.77	20.30	20.77		20.27
	22.21	21.74	22.21		21.71
	23.65	~~23.18~~	23.65		~~23.15~~
	~~25.09~~	24.62	~~25.09~~		24.59

2.2 Meteorological Data

Wind speeds were recorded at the Taylor Glacier meteorological station, one of twelve year-round stations deployed by the MCM LTER. The Taylor Glacier station is installed on the glacier surface 4 km up glacier from the terminus at an elevation of 334 m (Nylen et al., 2004). The station measures wind speed at 3 m above the glacier surface with an RM Young propeller-type monitor with a stated wind speed accuracy of 2% up to 60 m s^{-1} (Doran et al., 2002b). The sensor collects data every 4 seconds, which is averaged at 15 minute intervals and recorded by a Campbell Scientific CR10 data logger. Maximum wind speeds are the highest recorded wind speed over the 15 minute record interval.

2.3 ENDURANCE CTD Profiles

ENDURANCE was an autonomous underwater vehicle deployed under the ice in Lake Bonney in the 2008-2009 and 2009-2010 austral summer seasons. Additional details about the vehicle can be found in Stone et al. (2010). ENDURANCE performed CTD casts along a 100 m grid survey in WLB and a 25 m grid survey near the terminus of Taylor Glacier. CTD profiles presented here are from the 25 m grid survey performed on November 23-24, 2009. Vertical CTD profiles were made using a SeaBird SBE 19plusV2 SEACAT instrument with an accuracy of ±0.005°C and ±0.0005 S m^{-1}. The CTD sampled at 4 Hz and was deployed at a drop speed of ~0.4 m s^{-1}, resulting in a ~20 cm vertical distance between samples (Spigel et al., in revision).

2.4 LTER CTD Profiles

The MCM LTER performs several CTD casts at the center of WLB during each austral summer. This record extends back to 1993 and provides a long term record of the temperature, salinity, and density profiles in the lake. CTD casts were performed with a Seabird 25 CTD by the MCM LTER at the center of WLB every austral summer season since 1993. The instrument has an accuracy of ±0.001°C and ±0.0003 S m^{-1} and is deployed at a drop speed of ~1 m s^{-1} at a sampling rate of 8 Hz. CTD-calculated depth measurements from pressure are converted to actual depth measured with a calibrated wire according to the WLB-specific equation:

$$y = -0.0019x^2 + 1.0162x + 0.8106 \quad (1)$$

where x = CTD measured depth (m) and y = wire corrected depth (m). Practical salinity and density are calculated from temperature, conductivity, and pressure according to the WLB-specific modified UNESCO Equation of State for seawater (EOS80; Fofonoff and Millard, 1983) presented in Spigel and Priscu (1996).

2.5 Blood Falls Flow Records

No comprehensive records of Blood Falls flow events have been published since Keys (1979), who compiled a list of all known flow records from 1958-1978. The distinctive red-orange ice cone can only form during winter flow events when the brine can flow out on to the lake ice and freeze. In the summer, brine remains liquid at atmospheric pressure at temperatures greater than -6°C (Mikucki et al., 2015) and flows directly in to the open water of the lake moat via a narrow channel. Winter flow events are therefore defined as instances in which a red stain extending on to the terminal moraine and the lake ice is visible in imagery from satellites or historical photos. When the moat melts each summer, any brine on the lake ice enters the water column and no red coloration is left when the moat refreezes in the fall. Hence, the visual component of Blood Falls discharge is essentially “reset” each summer by the formation of the moat, and images of brine aprons in the spring and summer can confidently be assigned to the preceding winter (Figure 5). For the purpose of this record, “winter” refers to when the moat is fully frozen and ambient temperatures remain below the freezing point of the brine (approximately March – October). Keys (1979) measured discharge events by the volume of saline icing, so all recorded flow events from 1958-1978 are considered winter flow events with the exception of the active flow documented and sampled by Keys in November 1976.

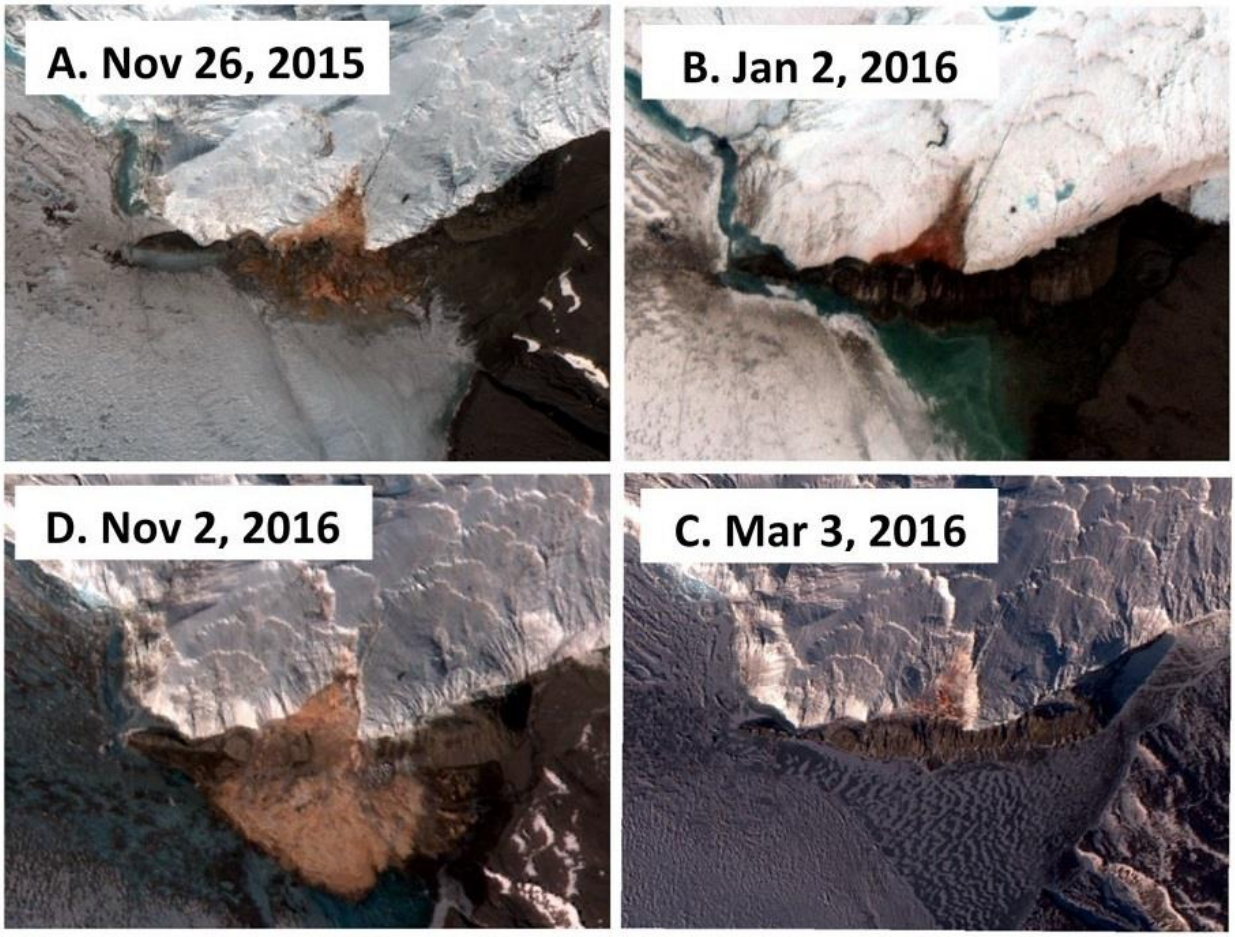

Figure 5. Clockwise from top left, satellite imagery shows how existing aprons of red brine on the moat ice (A) melt in to the moat during the summer (B). The new ice that forms in the fall (C) has no red coloration, and any brine aprons seen the following spring (D) must have occurred over the preceding winter.

High resolution satellite imagery from 2004-2016 was provided by the Polar Geospatial Center (PGC) at the University of Minnesota from DigitalGlobe satellites Quickbird-2, Worldview-2, and Worldview-3. Multispectral imagery was pansharpened to produce true-color images with average spatial resolutions of 0.66 m (Quickbird-2), 0.51 m (Worldview-2), and 0.36 m (Worldview-3). Visual interpretation of red staining in the Blood Falls region was used to indicate whether surface brine discharge had occurred the preceding winter. Visual interpretation of red staining was also performed on archival photos of Blood Falls when available on mcmurdohistory.lternet.edu.

Summer brine discharge events from Blood Falls were determined from the chemistry of the Blood Falls outflow. The MCM LTER has been sampling the stream flow emanating from Blood Falls every summer since 1993 (except for the 2006-2007 season). The stream is often dominated by glacial meltwater, but the presence of brine in the stream can be detected by a distinctive ionic ratio and high chloride concentrations. For the purpose of this record, we are defining summer brine flow events in the stream record when chloride concentrations exceed 90% of the total ion concentration by equivalence and the chloride concentration is greater than 10 g L^{-1}. At chloride concentrations <10 g L^{-1}, the ion ratios change significantly and are more representative of surface melt from the glacier (K. Welch, personal communication). Stream chemistry data is available at www.mcmlter.org. Ion concentrations were determined according to Welch et al. (1996). Sampling dates containing end-member brine are listed in Table 2 as summer Blood Falls flow events.

3. RESULTS

3.1 Thermal Variability of WLB from Over-Winter Thermistor Record

Temperature contour plots from all four thermistor locations are presented in Figure 6. Anomalously cold temperatures associated with brine inflow affect the water column between 18-23 m. A temperature anomaly is defined here as a disruption of the temperature stratification in the lake in which colder water overlies warmer water below the chemocline. Since the thermistors are spaced at 1.44 m intervals, this definition is conservative and other temperature anomalies that cannot be identified in this data set likely exist.

Temperature anomalies are colder and more frequent in the thermistor strings closest to the center of the glacier terminus (C and D). At Location C (2015-2016), minimum temperatures at the anomaly depths reached -3.1°C at 20.8 m. Temperature anomalies occur at 20.8 m at Location C for 70% of the year-long record, including a continuous five month period from December 2015 to May 2016. Temperature at 20.8 m at Location C is also the most variable in the record, with a temperature range of -0.7°C to -3.1°C and a standard deviation of 0.5°C, compared to an average standard deviation of 0.2°C for the other thermistors at Location C. At Location A (2014-2015), temperature anomalies reaching a minimum of -2.1°C occur for 16% of the record at 20.8 m. In contrast to Location C, the minimum temperature at Location A was recorded at 22.2 m, where the temperature reached -2.5°C. The standard deviations of temperature at 20.8 m and 22.2 m at Location A are 0.3°C and 0.2°C, respectively.

In the eastern thermistor strings (Locations B and D in Figure 4), temperatures between 18-23 m are warmer and less variable than in the western thermistor strings closer to the glacier (Locations A and C). Like Locations A and C, B and D are not directly comparable because the data was not collected simultaneously. At Location B (2014-2015), the furthest location from the glacier terminus, temperature anomalies occur for 8% of the record at 20.3 m, reaching a minimum temperature of -1.8°C. Location D (2015-2016) is colder and has a greater frequency of temperature anomalies than Location B, but is warmer overall than Location C to the west. Temperature anomalies occur for 8% of the record at 20.3 m and 10% of the record at 21.7 m at Location D, reaching a minimum temperature of -1.6°C at 20.3 and -2.1°C at 21.7 m. Because the thermistor at 23.1 m failed, the anomalies at 21.7 m are based off the temperature at 24.6 m and are likely underestimated. The standard deviation at 20.3 m is 0.2°C at both Locations B and D.

Mean temperatures at most of the thermistors below the chemocline do not exhibit linear trends over the course of the year. Mean temperatures during the first and last months of the record vary by less than 0.25°C at almost all depths. However, thermistors between 20-23 m depth at Locations A, C, and D show cooling trends over the course of the record. Mean temperatures at 20.8 m and 22.2 m at Location A fell by 0.6°C and 0.3°C, respectively, beginning in May 2015. A nearly constant temperature anomaly at Location C at 20.8 m lasted from December 2015 until July 2016 with a mean temperature of -2.0°C and minimum temperatures reaching -2.8°C in July 2016. Mean monthly temperatures at 20.3 m and 21.7 m at Location D declined by 0.5°C between May and November 2016 following the persistent temperature anomaly at 20.8 m at Location C (Figure 7). A CTD cast performed on November 22, 2016 at Location E shows that anomalously cold temperatures had reached the center of WLB and extended from 19-24 m (Figure 8). The minimum temperature was -1.9°C at 21.7 m.

3.2 Frequency Analysis of CTDs and Correlations with Surface Wind Speeds

Wavelet analysis of density at Location C shows significant wavelet power at periods less than an hour (Figure 9). Scale averaged wavelet power of density at 18 m and 23 m over 2-64 minute periods is shown in Figure 10 and demonstrates a strong correlation with maximum wind speeds at nearby Taylor Glacier Met Station. Variance has no direct linear relationship with maximum wind speeds, though all wind events with maximum wind speeds exceeding 26 m s^{-1} are correlated with significant wavelet power at 18 m. All other events with significant wavelet power at 18 m are correlated with wind events with maximum wind speeds of at least 18 m s^{-1}. Maximum scale averaged wavelet power occurred in late May 2016 during a katabatic event when maximum wind speeds exceeded 37 m s^{-1}. This event coincided with nearly isothermal conditions at Location C from 19.3-23 m (Figure 11).

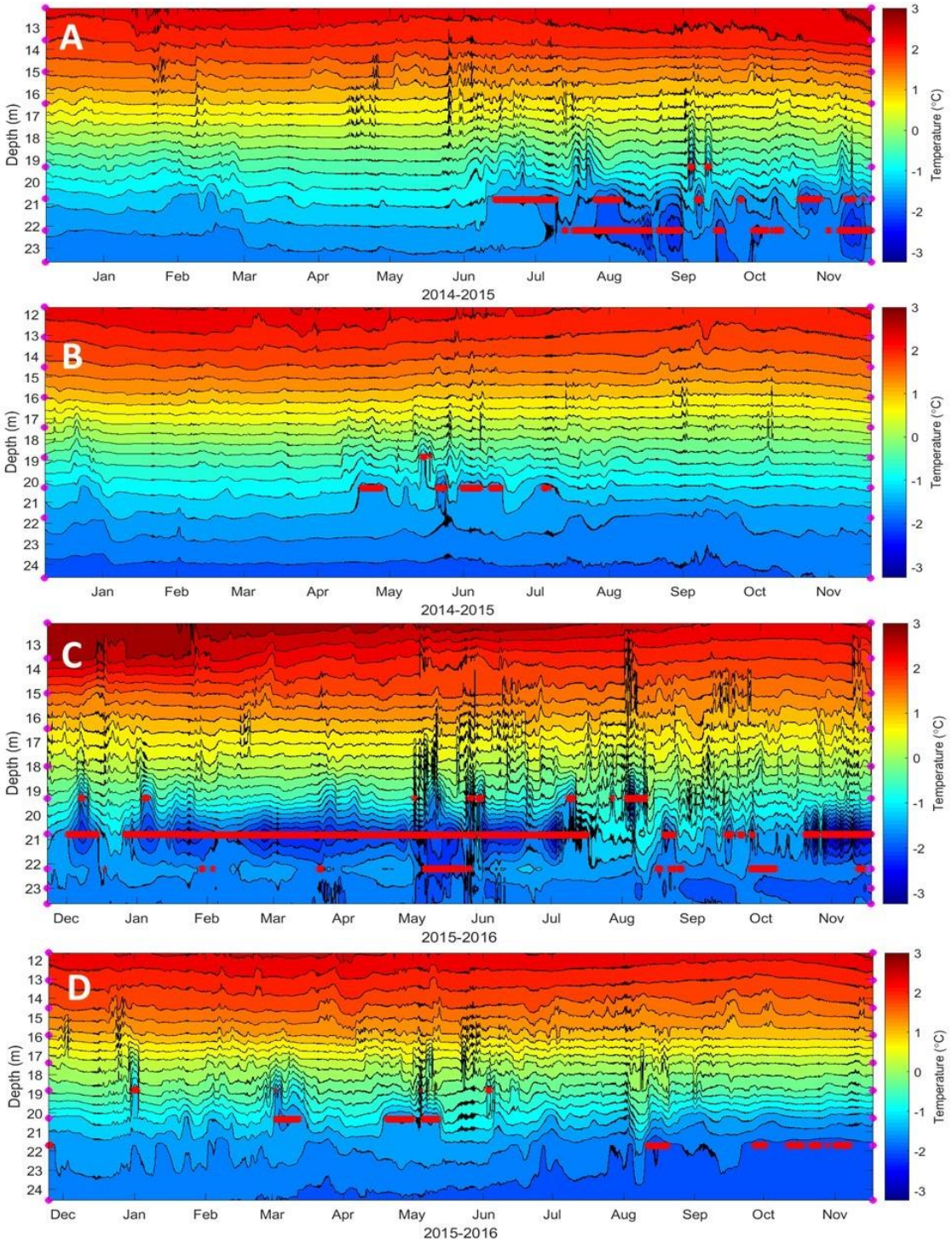

Figure 6. Temperature contour plots of the thermistor strings at each of the four locations from 2014-2016. See Figure 4 for their location on the map. Locations A and B (top) are the western and eastern locations (respectively) in 2014-2015. Locations C and D (bottom) are the western and eastern locations in 2015-2016. Sensor depths are indicated by pink dots on the y axis. The isotherm interval is 0.25°C. Temperature anomalies are marked as red stars at the depth of the thermistor where they occur.

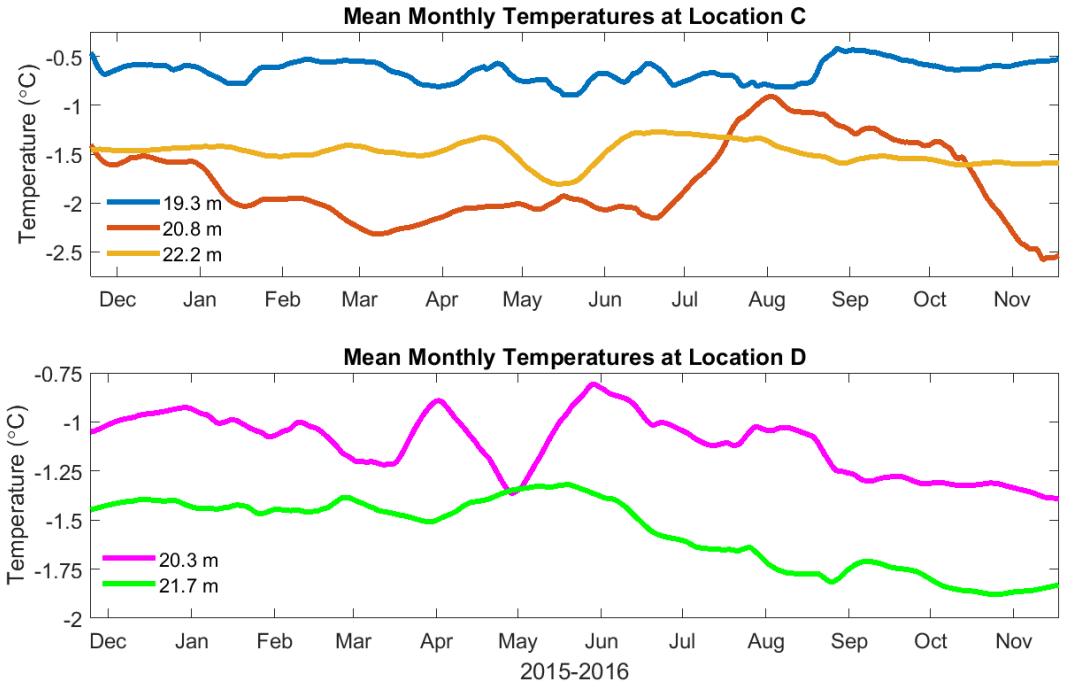

Figure 7. (Top) 30 day running average of temperatures at Location C at 19.3 m, 20.8 m, and 22.2 m. The mean temperature at 20.8 m is anomalously cold from December 2015 - July 2016. (Bottom) 30 day running average of temperature at 20.3 m and 21.7 m at Location D (100 m from Location C). Mean temperatures at both depths decrease by 0.5°C between May and November 2016.

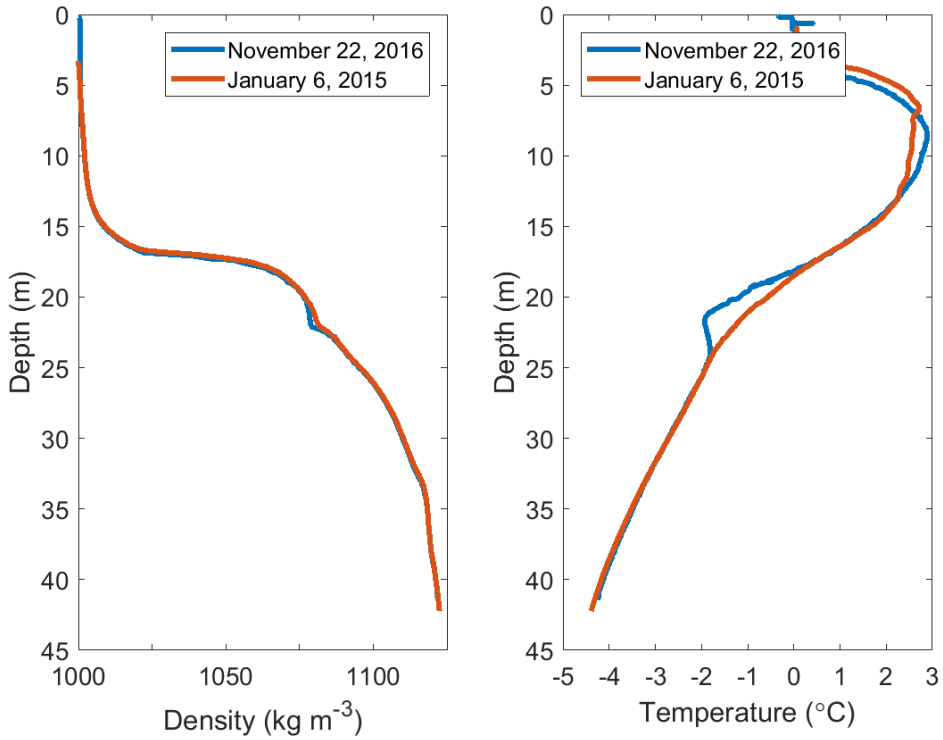

Figure 8. (Left) Density profiles at Location E on November 22, 2016 and January 6, 2015. (Right) Temperature profiles at Location E on November 22, 2016 and January 6, 2015.

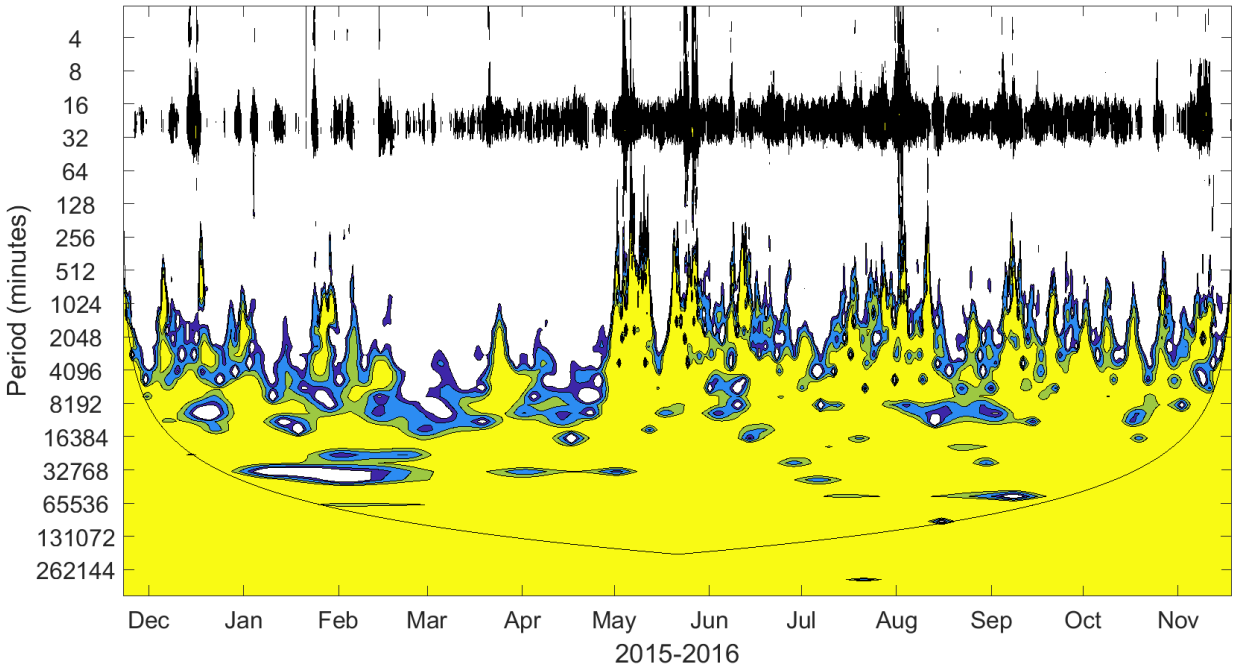

Figure 9. Normalized wavelet power spectrum using the Morlet wavelet of 1 minute density data from 18 m at Location C from 2015-2016. Contours are at normalized variances of 1, 2, 5, and 10. The black curve marks the cone of influence where edge effects become important.

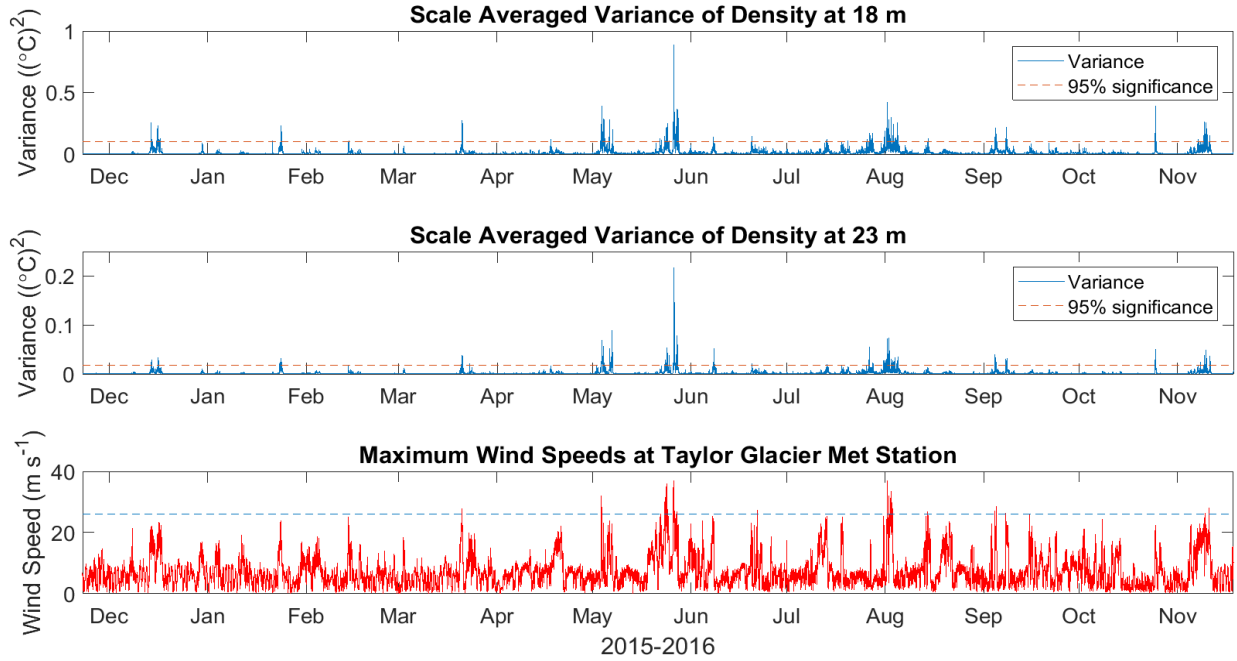

Figure 10. Scale averaged variance of density over periods of 2-64 minutes at 18 m (top) and 23 m (middle) at Location C is correlated with the maximum wind speeds at the nearby Taylor Glacier Met Station (bottom). All wind events with wind speeds exceeding 26 m s^{-1} (blue line) are correlated with significant wavelet power of density at 18 m.

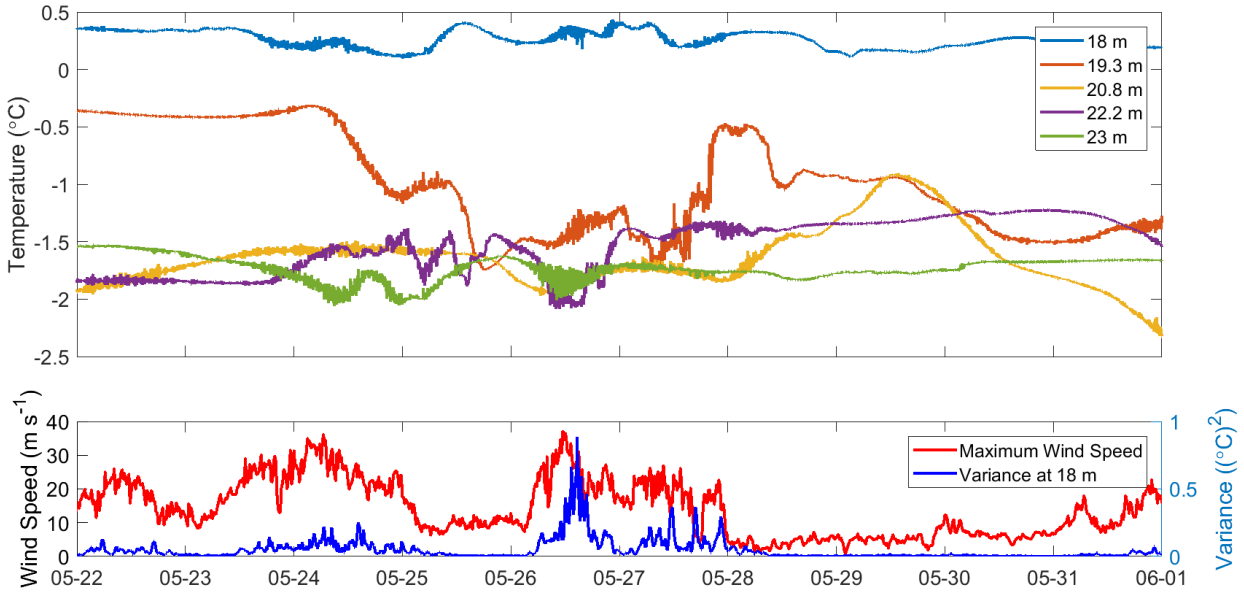

Figure 11. (Top) Temperature at Location C from in late May 2016. Temperatures between 19.3-23 m become nearly isothermal from May 25-27. (Bottom) Maximum wind speeds at Taylor Glacier met station and scale averaged variance from 2-64 minutes of density at 18 m at Location C. Variance reaches 0.88°C^2 on May 26, which is the maximum wavelet power in the entire annual record.

Wavelet power of density is also correlated with steep drops in temperature, or "brine pulses", that occur in the western thermistor string (Location C) shortly after strong winds subside. All instances in which scale averaged variance at 18 m from 2-64 minutes (Figure 10) exceeds 0.2°C^2 during the winter are correlated with a decrease in temperature of at least 0.5°C at one of the thermistors between 18-21 m within 48 hours of the wind event. The temperature decreases range from 0.5°C to 2°C and occur over a range of 1-6 days. With the exception of the katabatic event in late May 2016, all of the temperature decreases occurred at only one thermistor at either 18, 19.3, or 20.8 m. In late May 2016, the temperature decreases occurred at both the 19.3 and 20.8 m thermistors. Brine pulses occur at these depths at other times and are not always associated with wind or wavelet power. Figure 12 shows two examples of brine pulses in 2016.

3.3 Near-Glacier ENDURANCE CTD Profiles

The ENDURANCE AUV performed CTD casts in a 25 m spaced grid near Blood Falls and the Taylor Glacier terminus (Figure 13). All data presented here is from profiles performed on November 23-24, 2009. The temperature profiles in this region consistently show strong temperature anomalies at ~21 m depth. Many profiles exhibit an additional distinct cold anomaly below the chemocline between 16-19 m depth that is warmer and more variable than the cold anomaly seen at 21 m.

Figure 14 demonstrates the variability of temperature along the front of the glacier terminus. The minimum temperature observed near the glacier was -4.5°C at the southernmost point in the transect (BF45 in Figure 13). The temperature minimum occurred at the deepest part of the water column at BF45 at 17.5 m depth and is more than 4°C colder than the temperature at that depth elsewhere in the lake. Colder than average temperatures at BF45 (relative to other temperature profiles near the glacier) extend from ~12-17 m depth, though the salinity profile is typical at those depths. The depth of the lake along the glacier terminus remains shallow (<20 m) until BF40 (100 m north along the terminus), where a minimum temperature of -4.3°C occurs at ~21 m and the density profile becomes unstable from 20-21 m depth. The water column at BF40 between 18-20 m is cold (average temperature of -3.75°C) relative to other

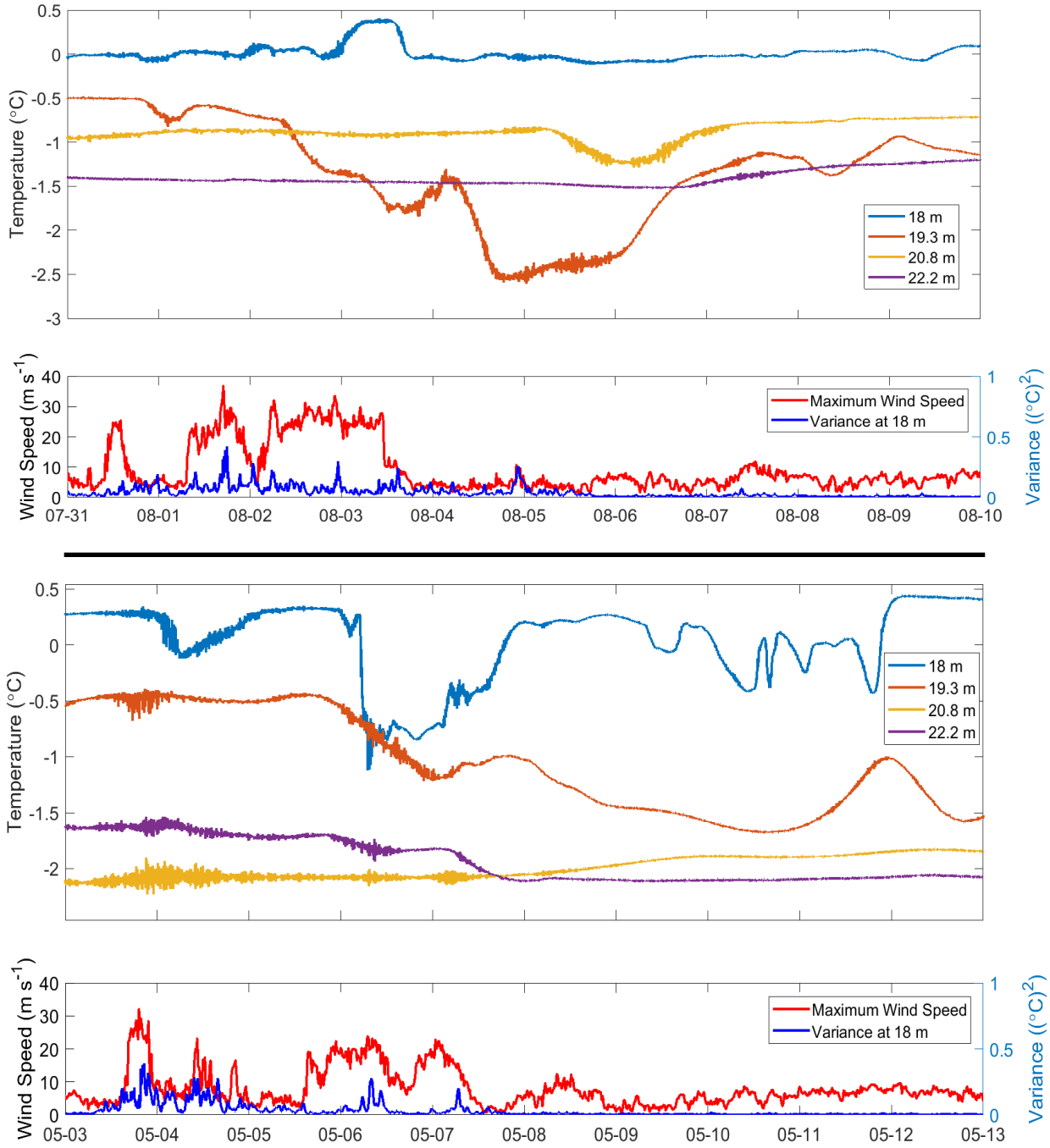

Figure 12. Brine pulses are shown as temperature decreases at Location C in August 2016 (top panels) and May 2016 (bottom panels) that are correlated with high winds at Taylor Glacier met station and high wavelet power over periods of 2-64 minutes at 18 m at Location C. In August 2016, temperature at 19.3 m decreased by 2°C between August 1 and August 4 after wind speeds reached 37 m s^{-1} and variance reached 0.42°C^2 on August 1. In May 2016, temperature at 19.3 m declined by 1.2°C between May 5 and May 10 after wind speeds reached 32 m s^{-1} and variance reached 0.38°C^2 on May 3. The 1.4°C temperature decrease at 18 m on May 6 may be an independent, faster moving brine pulse.

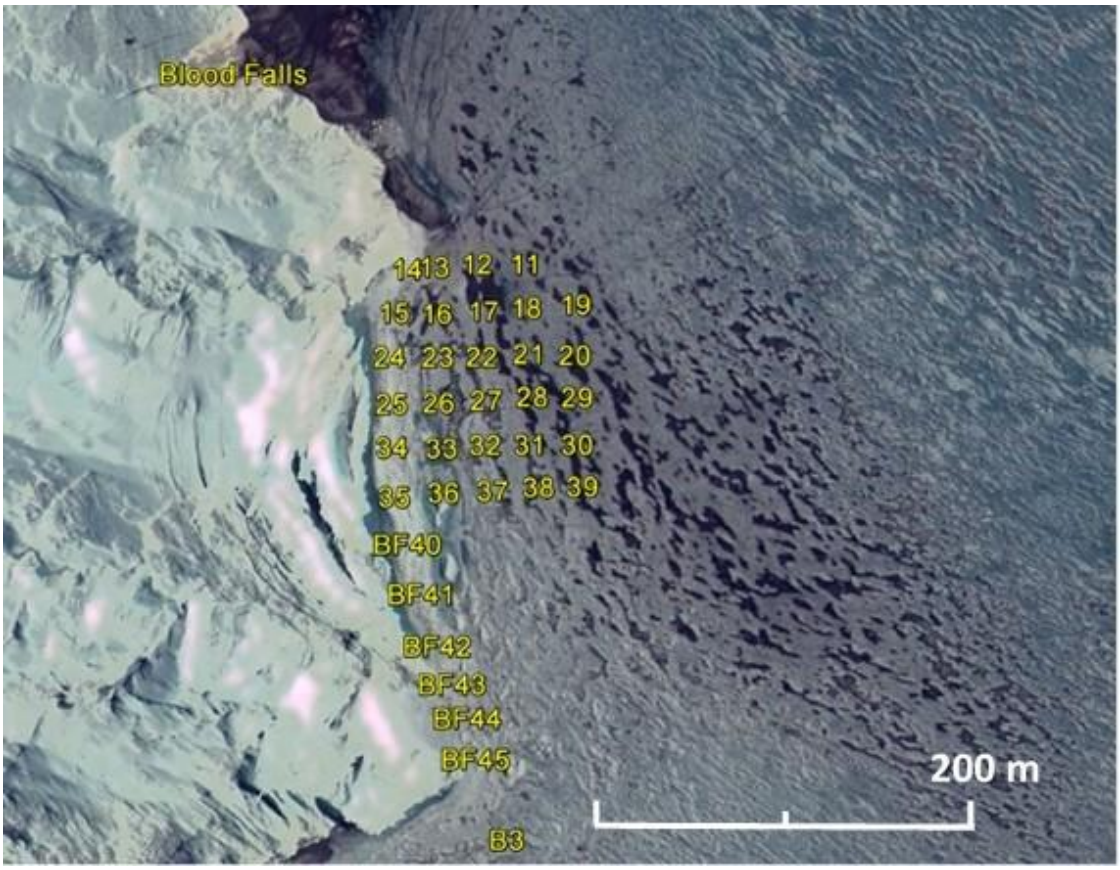

Figure 13. Map of sampling locations of the ENDURANCE AUV on November 23-24, 2009. Image from Google Earth (©2017 Google, DigitalGlobe).

locations in the lake, and salinity values are typical. The cold anomalies (reaching a minimum of -4.4°C) and density instabilities at 21 m persist for another 100 m north along the transect until the bathymetry of the lake becomes shallow again.

The east-west transects extending away from the glacier face show that the temperature anomaly persists for at least 100 m away from the terminus, though the anomaly weakens as the minimum temperature increases with distance from the glacier (Figure 15). Density instabilities at 21 m persist for at least 100 m away from the glacier face (Figure 16). The minimum temperature at 21 m along the east-west transects increases linearly with distance from the glacier at an average rate of 0.013°C m^{-1} (Figure 17).

3.4 Long Term LTER CTD Profiles

Cold temperature anomalies (defined as instances where temperature increases with depth below the chemocline) are present in many of the profiles since 1996 (Figure 18). The cold temperature anomalies are not correlated with density instabilities as seen in the near-glacier ENDURANCE profiles, but they are correlated with a shift in the density gradient towards isopycnal conditions at a lower density than usual at those depths (Figures 8 and 19).

The depth of the temperature anomalies in the water column (relative to sea level) has increased by approximately 4 m from 1996-2016. Lake level in WLB has risen by 3.6 m in the same time period. Lake level rise in WLB primarily thickens the freshwater layer above the chemocline, while the density stratification below the chemocline remains largely unchanged (Spigel and Priscu, 1996). Therefore, cold

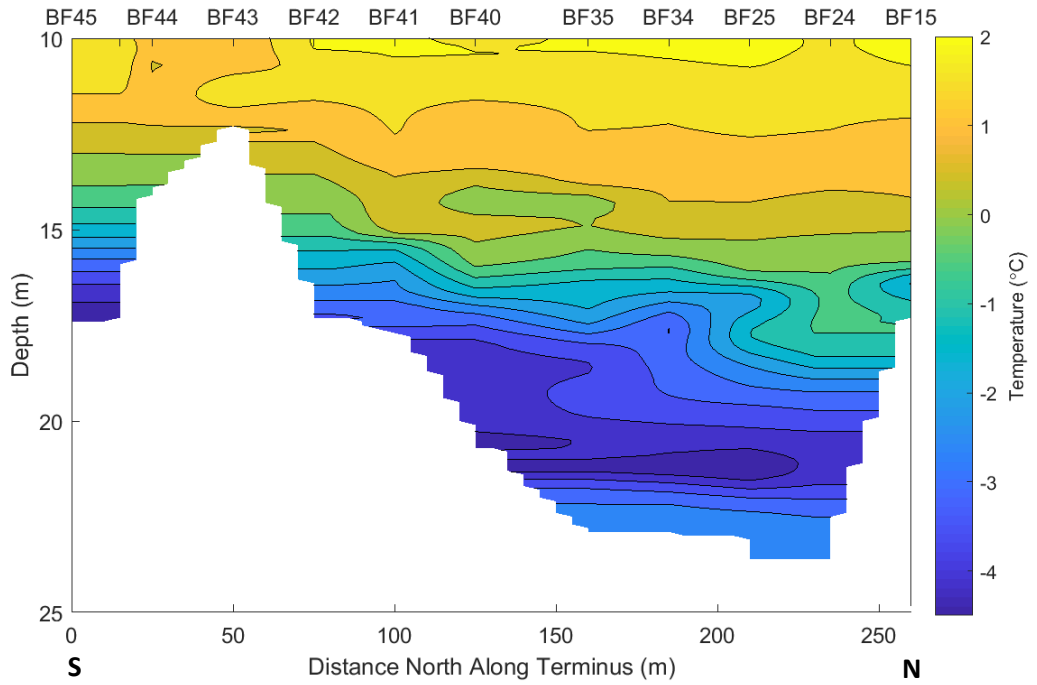

Figure 14. Temperature contour plot of a transect across the front of the terminus of Taylor Glacier from 10-25 m depth performed on November 23-24, 2009 by the ENDURANCE AUV. Isotherm intervals are 0.25°C. Sampling locations are listed at the top of the figure and correspond to sites in Figure 13.

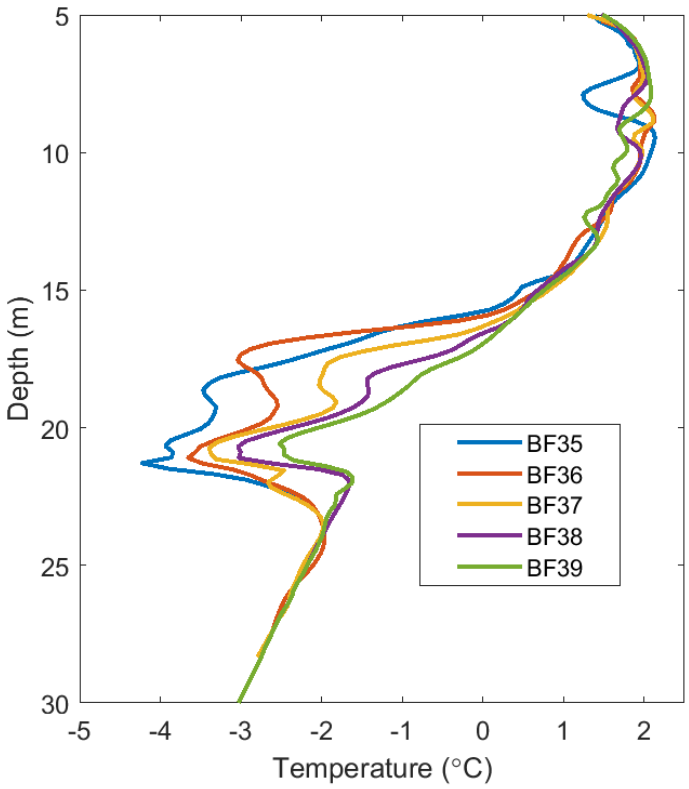

Figure 15. Temperature profiles from ENDURANCE CTD casts at four locations spaced 25 m apart, heading east away from the glacier face (BF35-BF39 in Figure 13). The temperature anomaly at 21 m diminishes with distance from the glacier face.

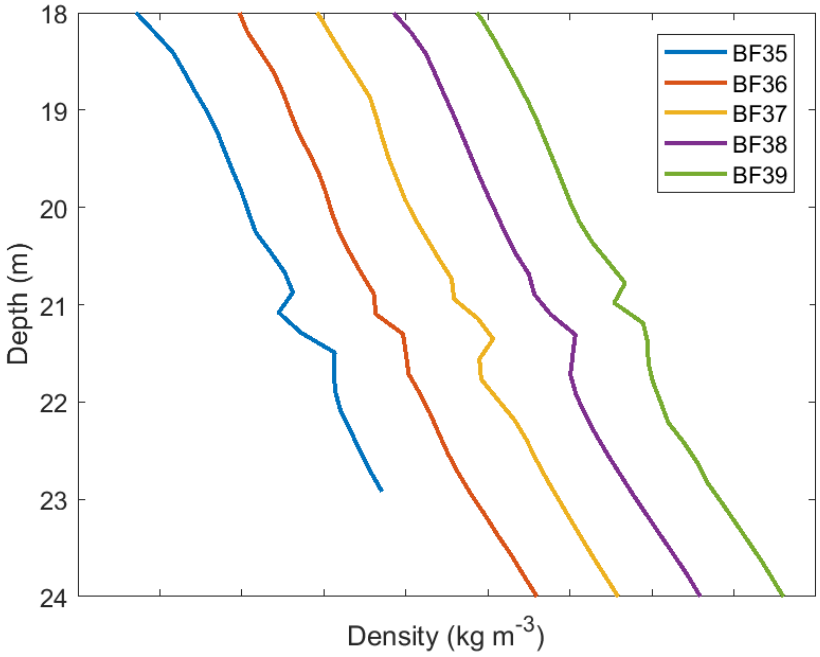

Figure 16. Density profiles from 18-24 m at locations BF35-39 (see Figure 13). The x-axis ticks and each profile are spaced 5 kg m^{-3} apart. Instability in the density profiles at 21 m persists to at least BF39, which is 100 m further from the glacier terminus than BF35. The instabilities occur where density is approximately 1080 kg m^{-3}.

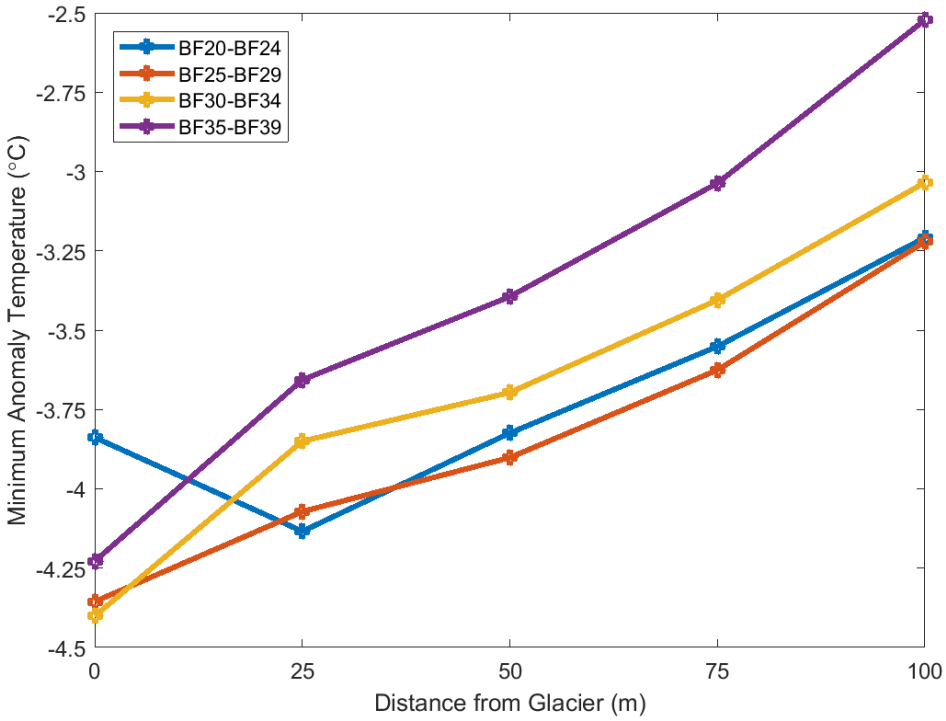

Figure 17. The minimum temperature of the temperature anomaly at 21 m from the ENDURANCE profiles performed on November 23-24, 2009 increases linearly with distance from the glacier face for at least 100 m. The average rate of warming is .013°C m^{-1}.

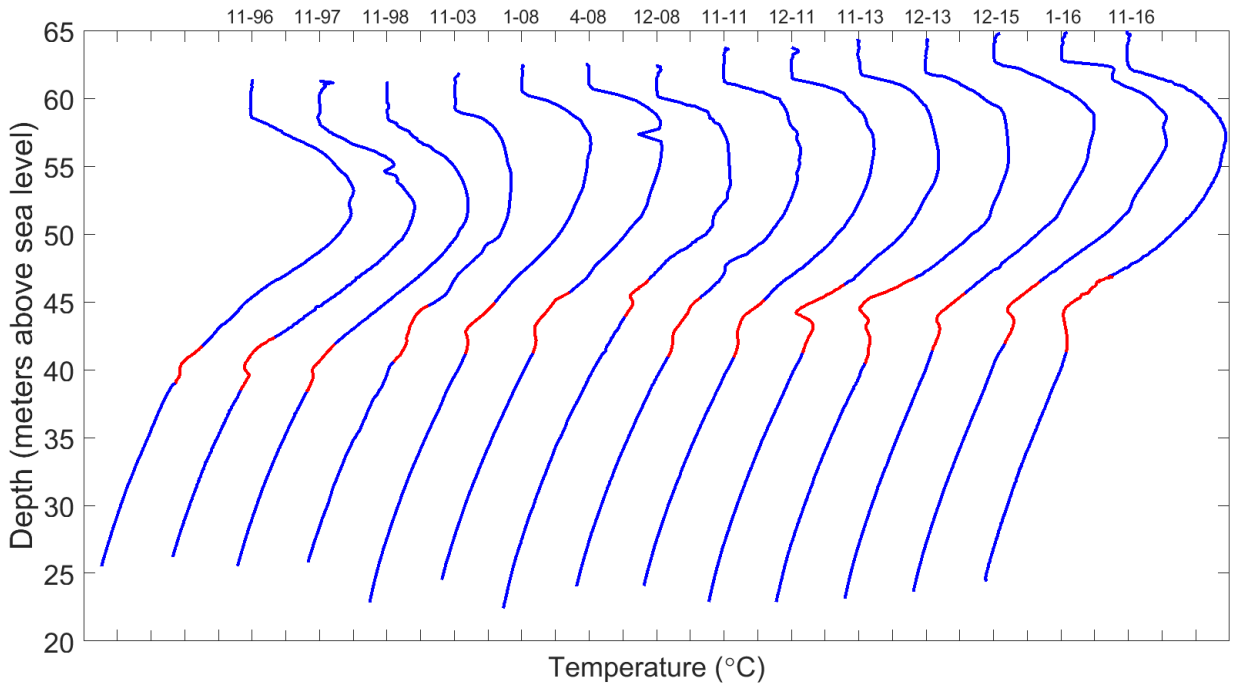

Figure 18. All temperature profiles from the long term LTER record that show cold temperature anomalies, where temperature increases with depth below the chemocline. The anomalous depths are highlighted in red. Profile months and years are listed at the top. X-axis ticks are spaced 1°C apart, and each profile is spaced 2°C apart.

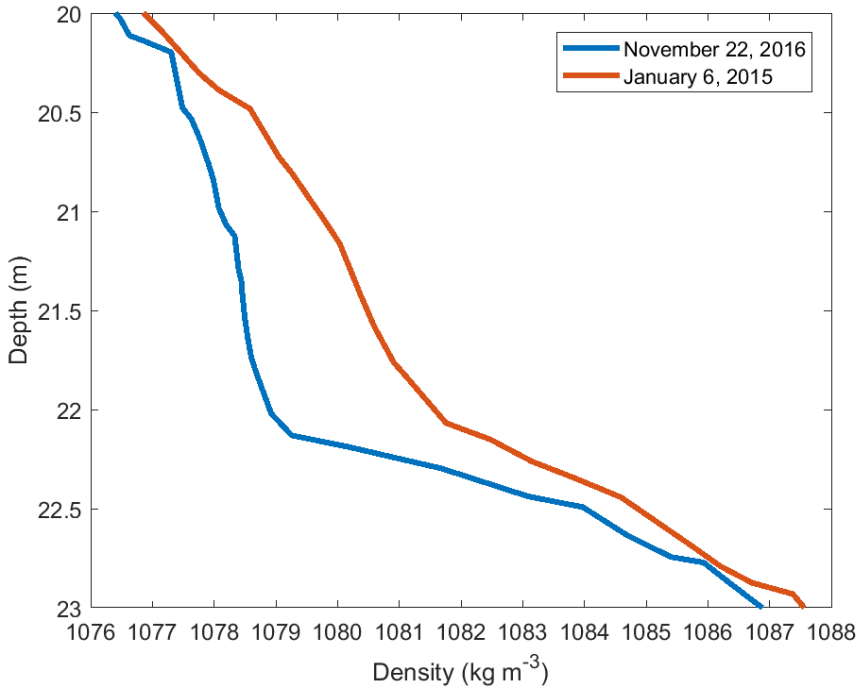

Figure 19. The shift in the density gradient between 20-23 m is correlated with cold temperature anomalies at the same depth. No temperature anomaly occurred on January 6, 2015, and a large temperature anomaly was present on November 22, 2016 (see Figure 8).

temperature anomalies that occur at a shallower depth below the chemocline indicate water masses of lower density than cold anomalies that occur deeper. Figure 20 illustrates the decrease in density at the depth of the temperature anomaly and the rough correlation with the rise in lake level since 1996. The lowest density associated with a temperature anomaly occurred in December 2008 during a period of abnormally high stream inflow from the surface. Satellite imagery from 2008 and 2015 indicates that the temperature anomaly only occurred at Location E in the center of WLB after the formation of the moat at the edges of WLB (2015 images shown in Figure 21).

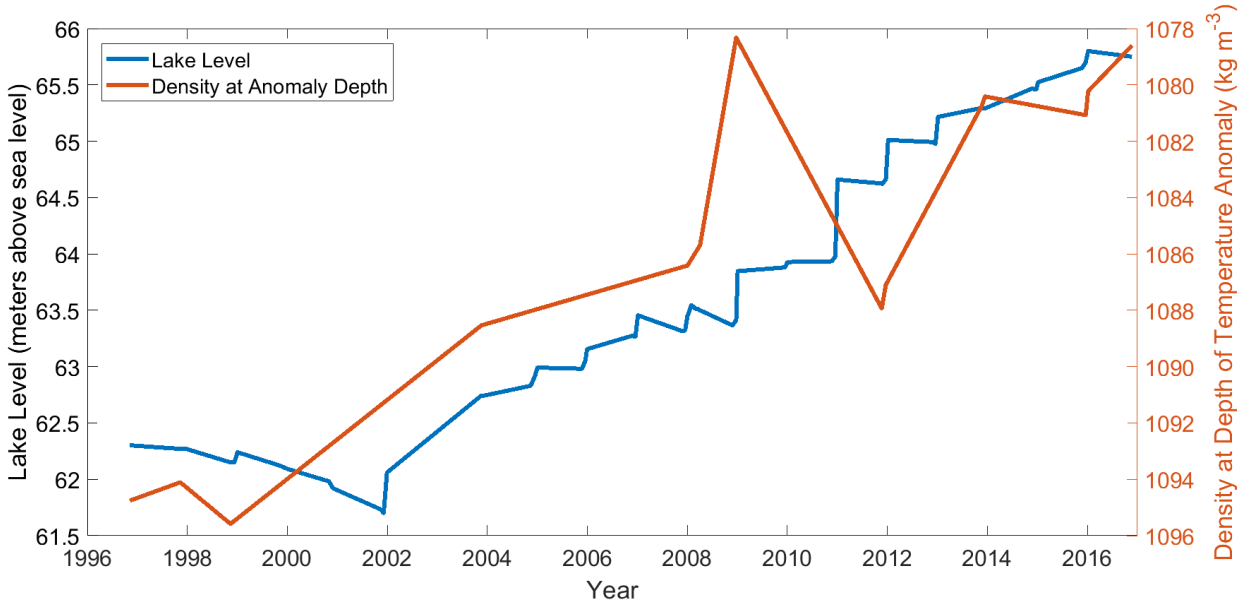

Figure 20. Lake level rise in WLB (blue) is roughly correlated with the decrease in density where temperature anomalies are found in the water column (orange). Note that the peak of low density in December 2008 occurred during a period of very high stream flow.

3.5 Blood Falls Flow Records

Table 2 combines the existing record of Blood Falls flow events with more recent data through 2016 to provide a more comprehensive historical record. Table 2 is not a complete record and it is likely that other flow events occurred and have not been recorded here, especially from 1980-1989 when there are no data reported. Blood Falls flow events in Table 2 are separated into summer and winter flow events. Table 2 includes the earliest available image each year that shows the red brine apron, meaning brine flow must have occurred sometime in the winter before that date.

The highest chloride concentration in the record is 58 g L^{-1} (94% Cl^- (meq)) in December 2011. The total dissolved solids (TDS) in the streamflow at that time was 98 g L^{-1}, significantly less than 133 g L^{-1} TDS of in-situ brine measured before it exited the glacier in 2014 (Lyons et al., in prep). Table 2 lists individual sampling dates that show a chemical signature of brine. The dates listed are sampling dates only and are not meant to imply that brine flow only occurred on those dates.

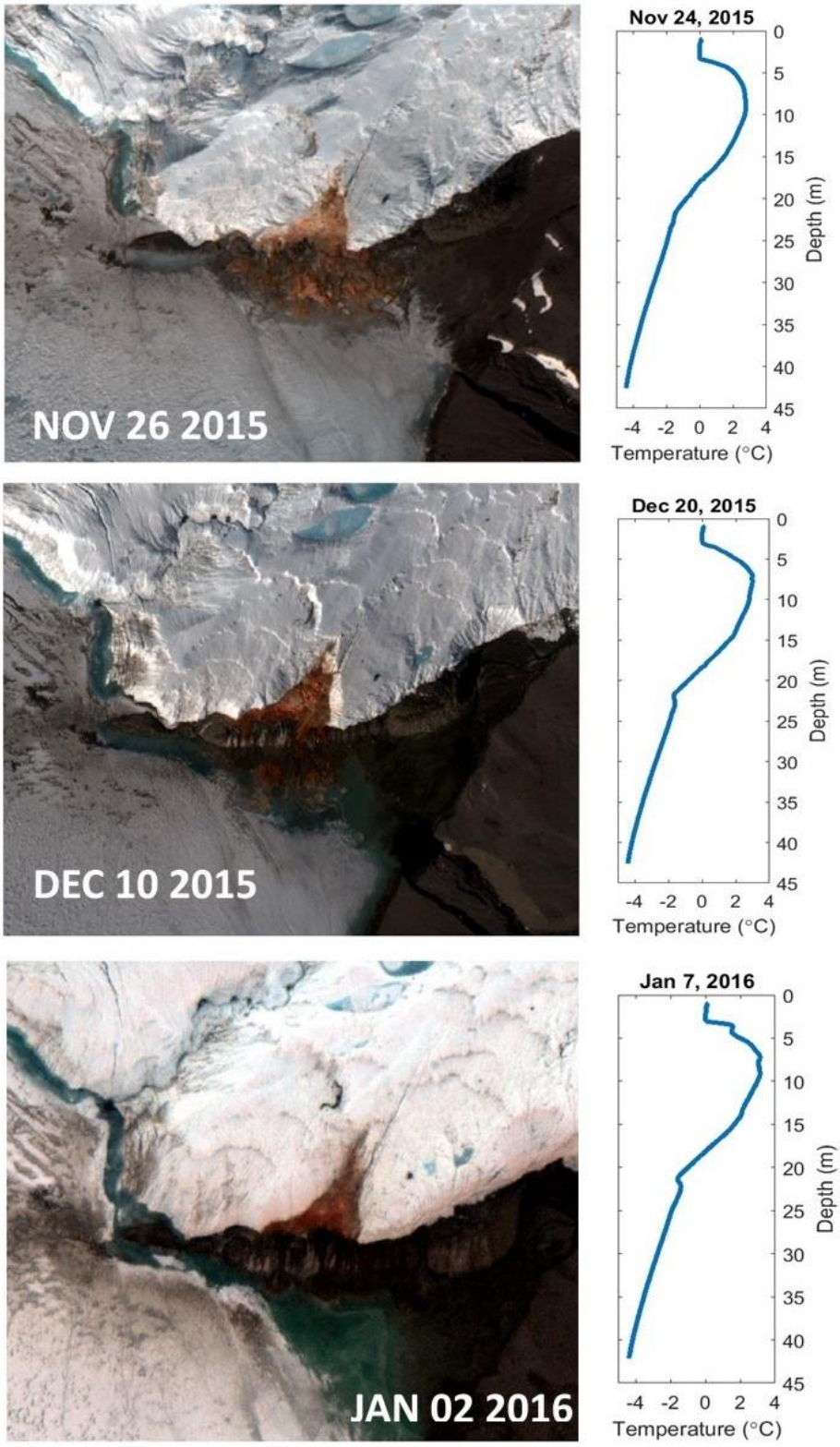

Figure 21. Satellite imagery from summer 2015-2016 shows that there was no temperature anomaly at Location E before the moat had melted in late November 2015 (top). A temperature anomaly occurred after the moat had opened in mid-December 2015 (middle) and strengthened by the time the remainder of the visible brine apron had melted into the moat in January 2016 (bottom).

Table 2. Known Blood Falls discharge events from 1911-2016. LTER refers to LTER sampling of Blood Falls outflow and includes the highest recorded chloride concentration each summer. Summer discharge events correspond to the austral summer beginning that year. Satellite images are listed with the corresponding DigitalGlobe satellite (QB02 = Quickbird-2, WV02 = Worldview-2) and the dates of the first image each season to show evidence of winter brine flow. Historical photos can be found with their identifiers at http://mcmurdohistory.lternet.edu/.

Year	Season	Observed flow dates	Maximum Cl^- conc. ($g\ L^{-1}$)	Earliest image with visible brine	Data Source
1911	winter				Taylor, 1922
1957	winter				Keys, 1979
1958	winter				Keys, 1979; historical photo (MCMEH-P001429)
1961	winter				Keys, 1979
1962	winter				Keys, 1979; Black, 1969
1967	winter				Keys, 1979
1968	winter				Keys, 1979; Black, 1969
1971	winter				Keys, 1979
1972	winter				Keys, 1979
1975	winter				Keys, 1979
1976	winter				Keys, 1979
	summer	November	65		Keys, 1979
1978	winter	ends in October			Keys, 1979
1990	summer	through at least January 1991			Spigel and Priscu, 1998
1991	winter	February-August 1991		unknown	Mikucki et al., 2004; historical photo (MCMEH-P000571)
1993	winter			11/21/1993	USGS aerial photos; historical photo (MCMEH-P000815)
	summer	12/20/1993; 1/19/1994	52		
1995	summer	12/1/1995; 12/29/1995	11		LTER
1996	winter			unknown	historical photo (MCMEH-P001195)
1997	summer	11/23/1997; 12/23/1997; 1/2/1998; 1/11/1998	48		LTER
1998	summer	1/19/1999; 1/17/1999	47		LTER
1999	summer	1/18/2000	50		LTER; Mikucki and Priscu, 2007
2001	summer	11/11/2001; 12/22/2001; 1/4/2002; 1/12/2002; 1/24/2002	51		LTER; Mikucki and Priscu, 2007
2004	winter			10/28/2004	Satellite image (QB02)
	summer	11/14/2004; 11/18/2004; 11/26/2004; 12/3/2004; 12/23/2004; 12/31/2004; 1/14/2005; 1/26/2005	51		LTER; Mikucki and Priscu, 2007
2007	summer	1/5/2008; 1/11/2008; 1/21/2008; 1/29/2008	56		LTER
2008	winter			10/25/2008	Satellite image (QB02)
2009	summer	12/24/2009; 12/27/2009; 1/8/2010; 1/15/2010; 1/22/2010; 2/5/2010	54		LTER
2010	winter			10/5/2010	Satellite image (QB02)
2011	summer	12/29/2011	58		LTER
2012	winter			12/16/2012	Satellite image (WV02)
2014	winter	5/12/2014- 6/7/2014			Infrared camera (E. Pettit, pers. comm.)
	summer	1/28/2015	11		LTER
2015	winter			10/26/2015	Satellite image (WV02)
2016	winter			9/21/2016	Satellite image (WV02)

4. DISCUSSION

4.1 Cold Temperature Anomalies as Evidence of Brine Intrusions

Because density is determined almost entirely by salinity in WLB, subglacial brine at neutral buoyancy will remain several degrees colder than the warmer water of equal density in WLB. The density of surface brine discharge at Blood Falls was calculated as 1100 kg m^{-3} in 1976 by Keys (1979). A 2014 sample of in-situ brine within the glacier had a TDS of 133 g L^{-1} (Lyons et al., in prep), which was converted to a density of 1106 kg m^{-3} (R. Spigel, personal communication; Spigel and Priscu, 1996). The similarity between the two values suggests that the density of brine at Blood Falls has not changed significantly over time. In WLB, cold temperature anomalies occur between 18-23 m depth, where the density of the water column ranges from 1060-1090 kg m^{-3}. Temperature anomalies associated with brine inflows are most commonly observed at depths where the density of the water column is near 1080 kg m^{-3}. The eventual density of brine inflows presumably depends on the degree of dilution with glacial melt and the amount of initial mixing as the brine enters the lake and migrates to the depth of neutral buoyancy. Cold temperature anomalies between 18-23 m depth can be attributed to brine inflows because of the similar density of the water column at those depths to Blood Falls brine, and because glacial meltwater below the chemocline does not behave in a way that would create similarly cold temperatures at those depths. Latent heat transfer from the melting face of Taylor Glacier results in colder temperatures in the water column of WLB near the terminus compared to the rest of the lake (Spigel et al., in revision). Glacial melt below the chemocline propagates into the lake as a series of nearly horizontal intrusions that are visible in fine-scale measurements as oscillations in the temperature and salinity with an average thickness of ~23 cm (Spigel et al., in revision). The meltwater intrusions quickly become stable with distance from the glacier face, and had largely decayed at a sampling site ~200 m away from the glacier face (Spigel et al., in revision). Large-scale intrusions of anomalously cold water can therefore be attributed to brine inflow rather than glacial melt.

Though subglacial brine entry has been proposed before (Spigel and Priscu, 1998; Doran et al., 2014; Badgeley et al., 2017; Spigel et al., in revision), evidence of brine inflow during the austral summer can be not be differentiated from surface brine inflows from Blood Falls due to the open water moat around the perimeter of the lake. The freezing of the moat during the winter months prevents hydrological connectivity between surface brine discharge at Blood Falls and the water column of WLB. Cold temperature anomalies that occur in the winter from the thermistor record must therefore come from a subglacial or englacial source below the ice cover of WLB.

4.2 Mechanisms for Brine Entry into WLB

Low resistivity values beneath Taylor Glacier established that the subglacial brine system is hydrologically connected to Blood Falls and to WLB (Mikucki et al., 2015). Badgeley et al. (2017) used hydraulic potential modeling to determine that subglacial brine in the northern half of the glacier terminus would be routed to a series of pressurized basal crevasses associated with Blood Falls, while subglacial brine in the southern half of the glacier terminus would flow directly in to Lake Bonney.

Badgeley et al. (2017) use hydraulic potential modeling routes subglacial brine in the southern half of the terminus region to the southern edge of the glacier approximately 500 m up glacier from WLB, and to a lesser degree directly in to Lake Bonney at the center of the terminus (Figure 22). Badgeley et al. concluded that the southern brine pathway would flow continuously and directly in to Lake Bonney instead of exiting at the sides of the glacier. Differences in surface topography such as smaller moraines, shorter ice cliffs, and more shallow surface valleys likely prevent a Blood Falls-like feature at the southern terminus (Badgeley et al., 2017). Ice-cored moraines and freezing of freshwater in proximal glacial sediments create physical barriers preventing brine outflow at the sides of the glacier terminus (Badgeley et al., 2017). The recurrent temperature anomaly at 20.8 m at Location C from 2015-2016 is likely a result of these southern and middle brine pathways that advect liquid brine pockets with glacier flow (3-4 m a^{-1}; Pettit et al., 2014) directly into Lake Bonney. Although the temperature records at Locations A and C are not directly comparable because they were not recorded simultaneously, the colder temperatures and increased variability at Location C suggest that the source of the cold temperatures is closer to Location C at the center of the glacier terminus rather than Location A near Blood Falls.

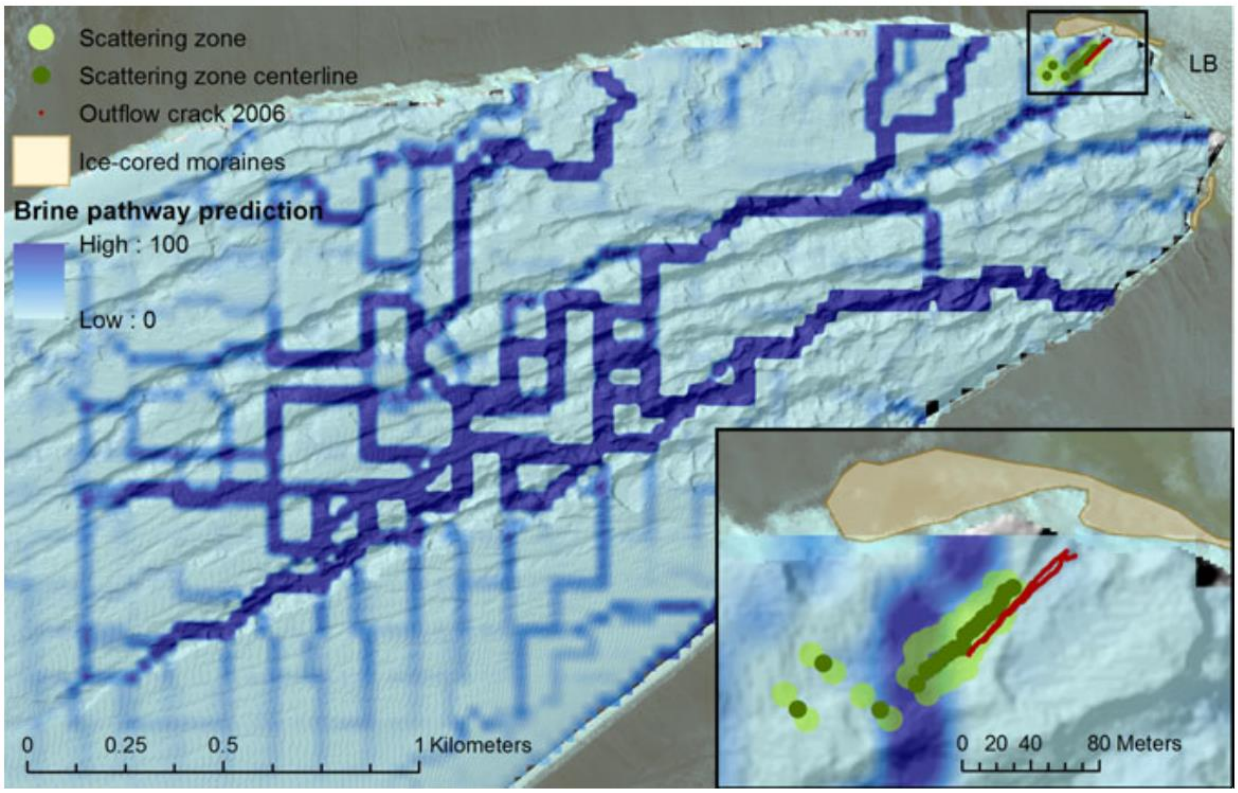

Figure 22. Subglacial brine pathways beneath Taylor Glacier predicted by hydraulic potential calculations. Brine in the northern half of the terminus will be routed towards Blood Falls, while brine from the southern and middle pathways will flow directly into WLB. Figure from Badgeley et al. (2017).

The near-glacier ENDURANCE profiles also suggest that brine is entering the lake from the southern end of the terminus (Figure 14). The abnormally cold temperatures at BF45 (the southernmost profile in the transect) coupled with typical salinity and density values could signify prior mixing with cold brine inflows that resulted in colder temperatures at BF45 after the density stratification was reestablished. Since liquid brine within Taylor Glacier has been measured at -7°C (Badgeley et al., 2017), temperatures within the water column approaching -5°C are reasonable for brine inflows that have entered the lake and mixed to some degree with the surrounding water. The initial mixing with glacial melt as brine enters the water column may result in a greater amount of turbulence and heat transfer than the subsequent entrainment of cold water from density driven flows down the side of the lake bed before the brine intrudes into the water column at the depth of neutral buoyancy. The abnormally cold temperatures and typical salinity values between 18-20 m at BF40 may similarly reflect mixing with brine that previously flowed north down the lake bed from a southern entry point near BF45.

In the northern subglacial brine pathway, subglacial brine is injected into a series of englacial basal crevasses and released at Blood Falls when a surface crevasse connects with the pressurized liquid brine in the basal crevasse (Badgeley et al., 2017). Smaller brine filled crevasses exist in a zone surrounding the primary Blood Falls outlet and are sometimes visible as red-orange streaks in the terminus cliff up to 150 m away (Badgeley et al., 2017). Smaller surface brine outflows have been observed at other locations near Blood Falls (Keys, 1979; Badgeley et al., 2017). The basal crevasses are another potential source of subsurface brine entry into WLB.

Surface brine discharge at Blood Falls also contributes brine to the water column during the summer. It is not known whether surface brine discharge contributes a greater volume of brine to the water column of WLB than subglacial inflows, or vice versa. Surface brine discharge will mix with variable

amounts of fresh water from glacial melt at the surface and in the water column before it sinks below the chemocline, and will therefore result in brine intrusions of variable densities and temperatures that intrude in to the water column at different depths. The decreasing density of the brine intrusions as lake level increased over time (Figure 20) suggests that the thickness of the water column above the chemocline contributes to the final density of surface brine inflows. Additionally, the "upper anomalies" that appear at shallower and more variable depths in the near-glacier ENDURANCE profiles (Figures 14 & 15) may be from small volumes of surface brine discharge at Blood Falls, or from an englacial source above the chemocline.

4.3 Internal Seiching below the Chemocline of WLB

The strong correlation between wind speeds and wavelet power of density at periods of less than an hour suggests that extreme katabatic winds initiate internal seiching beneath the chemocline in the deep waters of WLB (Figure 10). This finding contradicts the long held assumption that the thick perennial ice cover prevents wind induced mixing in Dry Valley lakes (Wharton, 1993; Spigel and Priscu, 1998). Though summer surface seiching has been observed in Lake Vanda (Heine, 1971), this is the first evidence of internal seiching occurring at depth during the winter in the Dry Valley lakes. Winter seiching has been observed in small freshwater lakes in Sweden and Russia caused either by wind forcing on the ice cover or variable air pressure fields (Bengtsson, 1996; Malm et al., 1998). The roughness of the ice cover over WLB's 1 km^2 surface (Wharton et al., 1993; Spigel and Priscu, 1998) could be a contributing factor in generating enough wind shear during katabatic events to induce seiching despite an ice thickness of 3-5 m.

In addition, winter seiching events are correlated with rapid temperature decreases at Location C at either the 18 m, 19.3 m, or 20.8 m thermistors that I interpret here as "brine pulses". Brine pulses are fast-moving, short lived phenomena of variable temperatures and salinities that appear at Location C within 48 hours of a peak in wavelet power. I infer that the cold temperatures are from a brine intrusion and not from entrainment of colder water in a mixing cell because the temperature of the brine pulse often becomes colder than the temperature at deeper thermistors, which do not appreciably change during the brine pulse (Figure 12). The exact mechanism between seiching and brine release is not clear, but it is possible that pressure changes at the glacier face caused by internal seiching could trigger brine release from the system of pressurized basal crevasses proposed in Badgeley et al. (2017). The brine pulses appear at variable depths and usually at a shallower depth than the most common brine inflow at 20.8 m, which supports the idea of brine release above the chemocline that mixes with freshwater before it sinks below the chemocline. Brine pulses are not correlated with wavelet power in the summer, when the open moat allows dissipation of the energy and pressure changes from seiching. Brine pulses occur at other times throughout the year and are not always correlated with high wind events or wavelet power.

4.4 Effect of Brine Intrusions on the Thermal and Density Stratification of WLB

The near-glacier ENDURANCE profiles (Figures 14-16) provide insight on the behavior of brine inflows as they enter the lake. Large temperature anomalies and density instabilities are present at 21 m in all of the profiles performed on November 23-24, 2009. Interpretations presented here assume that brine inflows at this depth occur at weeks-long time scales and that significant changes to the temperature and salinity structure of the lake did not occur over the sampling period. Therefore, the data presented here is intended as a 'snapshot' of the water column during a brine inflow event. The cold temperature anomalies (reaching a minimum of -4.4°C) and density instability at 21 m at all the profiles closest to the glacier are consistent with a recent brine inflow that is intruding into the water column at a depth where the density is ~1080 kg m^{-3}. The density instabilities suggest that the brine intrusion caused a turbulent mixing cell less than a meter thick to form at that depth (Figure 16). Because the density instability at 21 m persists across all of the near-glacier profiles, turbulent mixing of the brine intrusion with the surrounding water continues for at least 100 m away from the glacier face. The decay of the temperature anomaly (shown in Figure 17 as a linear increase in the minimum temperature of the anomaly) further supports the concept of cold brine inflows quickly warming as they mix with the warmer adjacent lake water of equal density. Once a stable density configuration is established at the depth of the

intrusion, the temperature anomaly will dissipate more slowly via diffusive heat transfer with the surrounding water.

The thermistor record at Location C from 2015-2016 confirms that brine inflows occur frequently at the same depth as seen in the ENDURANCE profiles. Temperature anomalies occur for 70% of the annual record at 20.8 m, which serves as a lower bound for the amount of time brine intrusions are present at that depth (Figure 6). Because Location C is only 150 m from the glacier face, it is possible that density instabilities from brine intrusions are still occurring at that point and could contribute to the high degree of variability seen in the temperatures at 20.8 m, though temperature data alone is insufficient to determine whether mixing is occurring. Temperature anomalies at the other thermistor locations (A, B, and D) are most common between 20.3-21.7 m, which is consistent with brine intrusions traveling laterally through the water column at a constant depth near 21 m and slowly cooling the water above and below the intrusion until thermal equilibrium is achieved.

The cold signature of brine intrusions is evident in the eastern thermistor string (Location D) as a decline in the mean temperatures at 20.3 and 21.7 m following the steady brine intrusion seen at 20.8 m at Location C (Figure 7). The decline in mean temperatures at those depths represents the “arrival” of the cold brine intrusion that lasted from December 2015 to July 2016 at Location C. The decline of mean temperatures from May – November 2015 at Location A may signal the beginning of a period of high brine inflow that continued in the record at Location C. Temperature data alone gives no indication of the volume of the brine inflow, so the movement of brine cannot be traced, nor can the amount of time that elapsed between cold brine appearing at Location C and at Location D be estimated. The brine enters the lake in liquid pockets that are advected with glacier flow (Badgeley et al., 2017), so brine release is probably episodic rather than a steady flow of constant volume. The large temperature anomaly in the CTD profile at Location E on November 22, 2016 (Figure 8) suggests that the brine inflow had extended to at least the center of WLB and affected 4 vertical meters of the water column.

The CTD profile at Location E on November 22, 2016 also exhibited lower densities than typical from 20 - 23 m (Figure 19). The weak density gradient between 21-22 m may be a remnant of a turbulent mixing cell that formed as the brine intruded at the glacier face and resulted in a layer of isopycnal water containing the cold temperature signal. The brine intrusion dissipates as it migrates laterally into the lake and the density gradient would eventually return to its typical profile. The difference between density profiles during a temperature anomaly and during conditions with typical temperature stratification may give some indication of the volume of brine inflow. A greater vertical distance in the water column with a weak density gradient would therefore indicate a high volume of brine inflow. The CTD profile performed on November 22, 2016 contains both the coldest temperature anomaly in the LTER record and the greatest difference in the density profile at that depth (Figure 8). 2015-2016 (beginning with the cold anomalies that appeared at Location A in the second half of 2015) may therefore have been a period of abnormally high volumes of subglacial brine flow that resulted in large temperature anomalies within a thick layer of weakly stratified water that persisted at least to the center of WLB (Location E). The slope of the density profile shifts slightly at 21 m even in years when no temperature anomaly is present, suggesting that brine inflows may have a cumulative effect on the density stratification of the water column over time.

Layers of weakly stratified water associated with brine intrusions may be susceptible to turbulent, wind-induced mixing during periods of internal seiching. Without salinity data and with the thermistors spaced at 1.44 m intervals, it is not possible to say whether the isothermal conditions represent turbulent mixing across the ~4 m vertical range or possibly other brine inflows intruding at different depths with similar temperatures. However, weak density stratification associated with brine inflows at Location E in the center of WLB suggests that the conditions may be met for a layer of isopycnal or weakly stratified water several meters thick at Location C closer to the source of brine inflows.

4.5 Brine Flow at Blood Falls and into WLB in the Long Term Record

Annual CTD casts performed annually since 1993 at Location E show that cold brine inflows reach the center of WLB frequently, but that the timing of those events is inconsistent and shows no discernible pattern (Figure 18). However, the open moat during the austral summer makes it impossible to differentiate between subglacial and surface brine entry in most of the profiles in the long term record.

The pattern of temperature anomalies occurring at shallower depths (relative to sea level) with time (Figure 20) suggests that the primary source of temperature anomalies in the historical record may be from surface brine discharge at Blood Falls. Lake level rise in WLB primarily thickens the freshwater layer above the chemocline, so brine entering the lake from Blood Falls at the surface would have to mix with increasing volumes of fresh water as it sinks below the chemocline. The resultant water mass would be less dense and would settle at a lower density and therefore shallower depth in the water column. The temperature anomaly with the lowest density and shallowest depth in the water column occurred in December 2008 during a period of very high streamflow. The additional mixing with incoming streamflow from streams adjacent to Blood Falls likely lowered the density of the resultant brine. Figure 21 shows a correlation between the opening of the moat around WLB and the appearance of temperature anomalies at Location E. In 2008 (not shown) and 2015 (Figure 21), temperature anomalies only appear at Location E after the brine apron on the lake ice has melted in to the moat.

However, temperature anomalies that occur in early November (1996, 1997, 1998) or after February (April 2008) are most likely unrelated to surface brine flow at Blood Falls because the frozen moat would prevent brine entry in to the water column. Additionally, the abnormally large temperature anomaly in November 2016 discussed above occurred despite a closed moat and a large brine apron as seen in a satellite image from December 7, 2016. Temperature anomalies in the austral summer at Location E are likely from a combination of surface and subglacial brine sources. Regardless, the persistence of anomalously cold water beneath the chemocline over a twenty year record demonstrates that there are frequent inputs of sufficient volumes of brine to affect the water column ~600 m away from the glacier face.

The record of Blood Falls flow events (Table 2) confirms that surface brine discharge has continued to occur frequently since the last record of flow events was published in 1979 (Keys, 1979). We make no attempt to measure the volume of brine discharge events, though estimated volumes for 1958-1978 can be found in Keys (1979) as the “volume of saline icing”. Satellite imagery could potentially be used to measure the extent of the red brine apron, but it is not known if the areal extent of brine flow is related to total brine volume discharged. In the summer record, the discrepancy between the highest recorded TDS in the summer record and the TDS measured from in-situ brine shows that even the most concentrated brine flows are diluted by glacial melt. Table 2 does demonstrate that brine discharge events are common both in summer and in winter. An infrared camera in 2014 (E. Pettit, personal communication) documented a winter flow event happening over the course of three weeks in May-June 2014, but the timing of other winter flow events is unknown. A camera taking daily photos of Blood Falls was installed on the shore of WLB in 2016 and will capture flow events that occur before and after the total darkness of polar winter. The persistence of Blood Falls as a site of significant brine discharge over the past 60 years (and potentially the last 100 years since Griffith Taylor in 1911) confirms its significance to the hydrology and geochemistry of the region.

5. CONCLUSIONS

This study is the first to demonstrate that brine enters WLB through subglacial sources independent of Blood Falls. Subglacial brine discharge is demonstrated through thermal evidence of brine intrusions during the winter, when the frozen moat ice prevents hydrological connectivity between surface brine discharge at Blood Falls and the water column of WLB. This study is also the first continuous record of subglacial brine intrusions and their effect on the thermal and density stratification of WLB. The prevalence of temperature anomalies in the continuous and long term records, as well as in the long term record of Blood Falls flow events, indicate that subglacial and surface brine release are ongoing processes that strongly affect the thermal structure and density stratification of WLB below the chemocline. Additionally, the discovery of wind-induced internal seiching in the winter is novel to Dry Valley lakes and challenges the assumption that the perennial ice cover provides an extremely stable environment that is not affected by surface processes in the winter. Seiching, and potentially turbulent mixing at the depth of the brine intrusions, has implications for nutrient transport and biological activity in WLB. The exact mechanisms controlling seiching events remains unclear and warrants future investigation.

Much remains unknown about the subglacial brine system and its effects on the WLB ecosystem. Subglacial brine discharge is biologically significant as a source of iron, DOC, and other nutrients in the winter. It is not known if the microbes in the subglacial brine can survive in the water column of WLB (Mikucki et al., 2004), though microbes with greater than 99% sequence similarity to Blood Falls isolates have been found at 16 m depth in WLB (Mikucki and Priscu, 2007) and the bacterial sizes of microbes from Blood Falls and the deep waters of WLB are similarly small compared to other Dry Valley lakes (Mikucki et al., 2004). Since the subglacial brine is anoxic and WLB is anoxic below the chemocline (Lizotte and Priscu, 1994), a subglacial pathway into the water column may allow the microbes to survive in anoxic conditions in WLB without exposure to oxygen via surface discharge at Blood Falls.

Future research should quantify the brine volume discharged and expand on the work of Badgeley et al. (2017) to explain the mechanisms controlling brine flow at Blood Falls and from subglacial sources. The volume of brine outflow is important in determining the geochemical history of the lake and for understanding the heat and salt budgets of WLB and ELB. The camera installed on the shore of WLB in 2016 will help assess whether surface brine flows at Blood Falls occur simultaneously with subglacial brine discharge. Evidence of subglacial brine discharge supports the finding of hydrological connectivity between the subglacial brine system, Blood Falls, and WLB proposed in Mikucki et al. (2015) and provides greater insight into this novel subglacial groundwater system.

REFERENCES

Badgeley, J. A., Pettit, E. C., Carr, C. G., Tulaczyk, S., Mikucki, J. A., & Lyons, W. B. (2017). An englacial hydrologic system of brine within a cold glacier: Blood Falls, McMurdo Dry Valleys, Antarctica. *Journal of Glaciology*, *63*(239), 387-400.

Bengtsson, L., Malm, J., Terzhevik, A., Petrov, M., Boyarinov, P., Glinsky, A., & Palshin, N. (1996). Field investigation of winter thermo-and hydrodynamics in a small Karelian lake. *Limnology and oceanography*, *41*(7), 1502-1513.

Black, R. F., Jackson, M. L., & Berg, T. E. (1965). Saline discharge from Taylor Glacier, Victoria Land, Antarctica. *The Journal of Geology*, 175-181.

Castendyk, D., McKnight, D., Welch, K., Niebuhr, S., & Jaros, C. (2015). Pressure-driven, shoreline currents in a perennially ice-covered, pro-glacial lake in Antarctica, identified from a LiCl tracer injected into a pro-glacial stream. *Hydrological processes*, *29*(9), 2212-2231.

Chinn, T. J. (1993). Physical hydrology of the dry valley lakes. In W. J. Green and E. I. Friedmann (Eds.), *Physical and Biogeochemical Processes in Antarctic Lakes* (pp. 1-51). Washington, DC: American Geophysical Union.

Clow, G. D., McKay, C. P., Simmons Jr, G. M., & Wharton Jr, R. A. (1988). Climatological observations and predicted sublimation rates at Lake Hoare, Antarctica. *Journal of Climate*, *1*(7), 715-728.

Cuffey, K. M., Conway, H., Gades, A., Hallet, B., Raymond, C. F., & Whitlow, S. (2000a). Deformation properties of subfreezing glacier ice: role of crystal size, chemical impurities, and rock particles inferred from in situ measurements. *Journal of Geophysical Research: Solid Earth*, *105*(B12), 27895-27915.

Dachwald, B., Mikucki, J., Tulaczyk, S., Digel, I., Espe, C., Feldmann, M., Francke, G., Kowalski, J., & Xu, C. (2014). IceMole: a maneuverable probe for clean in situ analysis and sampling of subsurface ice and subglacial aquatic ecosystems. *Annals of Glaciology*, *55*(65), 14-22.

Doran, P. T., Wharton, R. A., Des Marais, D. J., & McKay, C. P. (1998). Antarctic paleolake sediments and the search for extinct life on Mars. *Journal of Geophysical Research: Planets*, *103*(E12), 28481-28493.

Doran, P. T., McKay, C. P., Clow, G. D., Dana, G. L., Fountain, A. G., Nylen, T., & Lyons, W. B. (2002). Valley floor climate observations from the McMurdo Dry Valleys, Antarctica, 1986–2000. *Journal of Geophysical Research: Atmospheres*, *107*(D24).

Doran, P. T., Priscu, J. C., Lyons, W. B., Powell, R. D., Andersen, D. T., & Poreda, R. J. (2004). Paleolimnology of extreme cold terrestrial and extraterrestrial environments. In *Long-term environmental change in Arctic and Antarctic lakes* (pp. 475-507). Springer Netherlands.

Doran, P. T., Kenig, F., Knoepfle, J. L., Mikucki, J. A., & Lyons, W. B. (2014). Radiocarbon distribution and the effect of legacy in lakes of the McMurdo Dry Valleys, Antarctica. *Limnology and Oceanography*, *59*(3), 811-826.

Elston, D. P., & Bressler, S. L. (1981). Magnetic stratigraphy of DVDP drill cores and late Cenozoic history of Taylor Valley, Transantarctic Mountains, Antarctica. In L. D. Mcginnis (Ed.), *Dry valley drilling project* (pp. 413-426). Washington, DC: American Geophysical Union.

Fofonoff, N. P. & Millard, R. C. (1983). Algorithms for computation of fundamental properties of seawater. *UNESCO Technical Papers in Marine Science* (44). Paris, France: UNESCO Division of Marine Sciences.

Foreman, C. M., Wolf, C. F., & Priscu, J. C. (2004). Impact of episodic warming events. *Aquatic Geochemistry*, *10*(3-4), 239-268.

Fountain, A. G., Nylen, T. H., Monaghan, A., Basagic, H. J., & Bromwich, D. (2010). Snow in the McMurdo dry valleys, Antarctica. *International Journal of Climatology*, *30*(5), 633-642.

Hall, C. M., Castro, M. C., Kenig, F., & Doran, P. T. (2017). Constraining the recent history of the perennially ice-covered Lake Bonney, East Antarctica using He, Kr and Xe concentrations. *Geochimica et Cosmochimica Acta*, *209*, 233-253.

Heine, A. J. (1971). Seiche observations at Lake Vanda, Victoria Land, Antarctica. *New Zealand Journal of Geology and Geophysics*, *14*(3), 597-599.

Hendy, C. H. (2000). Late Quaternary lakes in the McMurdo Sound region of Antarctica. *Geografiska Annaler: Series A, Physical Geography*, *82*(2-3), 411-432.

Hoare, R. A., Popplewell, K. B., House, D. A., Henderson, R. A., Prebble, W. M., & Wilson, A. T. (1964). Lake Bonney, Taylor Valley, Antarctica: a natural solar energy trap. *Nature*, *202*, 886-888.

Holt, J. W., Peters, M. E., Kempf, S. D., Morse, D. L., & Blankenship, D. D. (2006). Echo source discrimination in single-pass airborne radar sounding data from the Dry Valleys, Antarctica: Implications for orbital sounding of Mars. *Journal of Geophysical Research: Planets*, *111*(E6).

Hubbard, A., Lawson, W., Anderson, B., Hubbard, B., & Blatter, H. (2004). Evidence for subglacial ponding across Taylor Glacier, Dry Valleys, Antarctica. *Annals of Glaciology*, *39*(1), 79-84.

Kavanaugh, J. L., & Cuffey, K. M. (2009). Dynamics and mass balance of Taylor Glacier, Antarctica: 2. Force balance and longitudinal coupling. *Journal of Geophysical Research: Earth Surface*, *114*(F4).

Keys, J. R. (1979). Saline discharge at the terminus of the Taylor Glacier. *Antarctic Journal of the US*, *14*, 82-85.

Lizotte, M. P., & Priscu, J. C. (1994). Natural fluorescence and quantum yields in vertically stationary phytoplankton from perennially ice-covered lakes. *Limnology and Oceanography*, *39*(6), 1399-1410.

Lyons, W. B., Welch, K. A., & Sharma, P. (1998). Chlorine-36 in the waters of the McMurdo Dry Valley lakes, southern Victoria Land, Antarctica: revisited. *Geochimica et Cosmochimica Acta*, *62*(2), 185-191.

Lyons, W. B., Welch, K. A., Snyder, G., Olesik, J., Graham, E. Y., Marion, G. M., & Poreda, R. J. (2005). Halogen geochemistry of the McMurdo Dry Valleys lakes, Antarctica: clues to the origin of solutes and lake evolution. *Geochimica et Cosmochimica Acta*, *69*(2), 305-323.

Lyons, W.B. (2017) *The Geochemistry of the Taylor Glacier Englacial Brine.* Manuscript in preparation.

Malm, J., Bengtsson, L., Terzhevik, A., Boyarinov, P., Glinsky, A., Palshin, N., & Petrov, M. (1998). Field study on currents in a shallow, ice-covered lake. *Limnology and oceanography*, *43*(7), 1669-1679.

Marchant, D. R., Denton, G. H., Sugden, D. E., & Swisher III, C. C. (1993). Miocene glacial stratigraphy and landscape evolution of the western Asgard Range, Antarctica. *Geografiska Annaler. Series A. Physical Geography*, 303-330.

Mikucki, J. A., Foreman, C. M., Sattler, B., Lyons, W. B., & Priscu, J. C. (2004). Geomicrobiology of Blood Falls: an iron-rich saline discharge at the terminus of the Taylor Glacier, Antarctica. *Aquatic Geochemistry*, *10*(3-4), 199-220.

Mikucki, J. A., & Priscu, J. C. (2007). Bacterial diversity associated with Blood Falls, a subglacial outflow from the Taylor Glacier, Antarctica. *Applied and Environmental Microbiology*, *73*(12), 4029-4039.

Mikucki, J. A., Pearson, A., Johnston, D. T., Turchyn, A. V., Farquhar, J., Schrag, D. P., Anbar, A. D., Priscu, J. C., & Lee, P. A. (2009). A Contemporary Microbially Maintained Subglacial Ferrous "Ocean". *Science*, *324*(5925), 397-400.

Mikucki, J. A., Auken, E., Tulaczyk, S., Virginia, R. A., Schamper, C., Sørensen, K. I., Doran, P. T., Dugan, H., & Foley, N. (2015). Deep groundwater and potential subsurface habitats beneath an Antarctic dry valley. *Nature communications*, *6*.

Nylen, T. H., Fountain, A. G., & Doran, P. T. (2004). Climatology of katabatic winds in the McMurdo dry valleys, southern Victoria Land, Antarctica. *Journal of Geophysical Research: Atmospheres*, *109*(D3), 1-9.

Obryk, M. K., Doran, P. T., Hicks, J. A., McKay, C. P., & Priscu, J. C. (2016). Modeling the thickness of perennial ice covers on stratified lakes of the Taylor Valley, Antarctica. *Journal of Glaciology*, *62*(235), 825-834.

Paren, J. G., & Walker, J. C. (1971). Influence of limited solubility on the electrical and mechanical properties of ice. *Nature*, *230*(12), 77-79.

Paterson, W. S. B. (1991). Why ice-age ice is sometimes "soft". *Cold Regions Science and Technology*, *20*(1), 75-98.

Pettit, E. C., Whorton, E. N., Waddington, E. D., & Sletten, R. S. (2014). Influence of debris-rich basal ice on flow of a polar glacier. *Journal of Glaciology*, *60*(223), 989-1006.

Poreda, R. J., Hunt, A. G., Lyons, W. B., & Welch, K. A. (2004). The helium isotopic chemistry of Lake Bonney, Taylor Valley, Antarctica: Timing of late Holocene climate change in Antarctica. *Aquatic Geochemistry*, *10*(3-4), 353-371.

Robinson, P. H. (1984). Ice dynamics and thermal regime of Taylor glacier south Victoria land, Antarctica. *Journal of Glaciology*, *30*(105), 153-160.

Scott, R. F. (1905). *The voyage of the Discovery (Vol 2).* London, England: Smith, Elder & Co.

Shirtcliffe, T. G. L., & Benseman, R. F. (1964). A sun-heated antarctic lake. *Journal of Geophysical Research*, *69*(16), 3355-3359.

Siegert, M. J., Kennicutt, M. C., & Bindschadler, R. A. (Eds.). (2013). *Antarctic subglacial aquatic environments* (Vol. 192). John Wiley & Sons.

Spigel, R. H., & Priscu, J. C. (1996). Evolution of temperature and salt structure of Lake Bonney, a chemically stratified Antarctic lake. *Hydrobiologia*, *321*(3), 177-190.

Spigel, R. H., & Priscu, J. C. (1998). Physical limnology of the McMurdo Dry Valleys lakes. In *Ecosystem Dynamics in a Polar Desert: The McMurdo Dry Valleys, Antarctica* (pp. 153-187). American Geophysical Union.

Spigel, R. H., Priscu, J. C., Stone, W., Obryk, M. K., Febretti, A., & Doran, P. T. (2017) *The Physical Limnology of a Permanently Ice-Covered and Chemically Stratified Antarctic Lake Using High Resolution Spatial Data from an Autonomous Underwater Vehicle.* Manuscript in revision.

Stone, W., Hogan, B., Flesher, C., Gulati, S., Richmond, K., Murarka, A., Kuhlman, G., Sridharan, M., Siegel, V., Price, R. M., Doran, P. T., & Priscu, J. C. (2010). Design and deployment of a four-degrees-of-freedom hovering autonomous underwater vehicle for sub-ice exploration and mapping. *Proceedings of the Institution of Mechanical Engineers, Part M: Journal of Engineering for the Maritime Environment*, *224*(4), 341-361.

Taylor, T. G. (1922). *The physiography of the McMurdo Sound and Granite Harbour region*. High Wycombe, United Kingdom: Harrison and sons, Ltd.

Torrence, C., & Compo, G. P. (1998). A practical guide to wavelet analysis. *Bulletin of the American Meteorological society*, *79*(1), 61-78.

Vincent, W. F. (1981). Production Strategies in Antarctic Inland Waters: Phytoplankton Eco-Physiology in a Permanently Ice-Covered Lake. *Ecology*, *62*(5), 1215-1224.

Welch, K. A., Lyons, W. B., Graham, E., Neumann, K., Thomas, J. M., & Mikesell, D. (1996). Determination of major element chemistry in terrestrial waters from Antarctica by ion chromatography. *Journal of Chromatography A*, *739*(1-2), 257-263.

Wharton, R. A., Mckay, C. P., Clow, G. D., & Andersen, D. T. (1993). Perennial ice covers and their influence on Antarctic lake ecosystems. In W. J. Green and E. I. Friedmann (Eds.), *Physical and Biogeochemical Processes in Antarctic Lakes* (pp. 53-70). Washington, DC: American Geophysical Union.

VITA

Jade Lawrence, a native of San Diego, California, received her bachelor's degree in biology from the University of California, Santa Barbara, in 2012. She then spent several years working on lakes in arctic Alaska before coming to LSU to study Antarctic lakes. Her research interests include very cold lakes and high latitudes.